JACS
JOURNAL OF THE AMERICAN CHEMICAL SOCIETY
Article
pubs.acs.org/JACS

Activation of B−H, Si−H, and C−F Bonds with Tp′Rh(PMe$_3$) Complexes: Kinetics, Mechanism, and Selectivity

Barbara Procacci,[†] Yunzhe Jiao,[‡] Meagan E. Evans,[‡] William D. Jones,*[,‡] Robin N. Perutz,*[,†] and Adrian C. Whitwood[†]

[†]Department of Chemistry, University of York, York YO10 5DD, U.K.
[‡]Department of Chemistry, University of Rochester, Rochester, New York 14627, United States

Supporting Information

ABSTRACT: The photochemical reactions of Tp′Rh(PMe$_3$)H$_2$ (**1**) and thermal reactions of Tp′Rh(PMe$_3$)(CH$_3$)H (**1a**, Tp′ = tris(3,5-dimethylpyrazolyl)borate) with substrates containing B−H, Si−H, C−F, and C−H bonds are reported. Complexes **1** and **1a** are known activators of C−H bonds, including those of alkanes. Kinetic studies of reactions with HBpin and PhSiH$_3$ show that photodissociation of H$_2$ from **1** occurs prior to substrate attack, whereas thermal reaction of **1a** proceeds by bimolecular reaction with the substrate. Complete intramolecular selectivity for B−H over C−H activation of HBpin (pin = pinacolate) leading to Tp′Rh(PMe$_3$)(Bpin)H is observed. Similarly, the reaction with Et$_2$SiH$_2$ shows a strong preference for Si−H over C−H activation, generating Tp′Rh(PMe$_3$)(SiEt$_2$H)H. The Rh(Bpin)H and Rh(SiEt$_2$H)H products were stable to heating in benzene in accord with DFT calculations that showed that reaction with benzene is endoergic. The intramolecular competition with PhSiH$_3$ yields a ∼1:4 mixture of Tp′Rh(PMe$_3$)(C$_6$H$_4$SiH$_3$)H and Tp′Rh(PMe$_3$)(SiPhH$_2$)H, respectively. Reaction with pentafluoropyridine generates Tp′Rh(PMe$_3$)(C$_5$NF$_4$)F, while reaction with 2,3,5,6-tetrafluoropyridine yields a mixture of C−H and C−F activated products. Hexafluorobenzene proves unreactive. Crystal structures are reported for B−H, Si−H, and C−F activated products, but in the latter case a bifluoride complex Tp′Rh(PMe$_3$)(C$_5$NF$_4$)(FHF) was crystallized. Intermolecular competition reactions were studied by photoreaction of **1** in C$_6$F$_6$ with benzene and another substrate (HBpin, PhSiH$_3$, or pentafluoropyridine) employing *in situ* laser photolysis in the NMR probe, resulting in a wide-ranging map of kinetic selectivities. The mechanisms of intramolecular and intermolecular selection are analyzed.

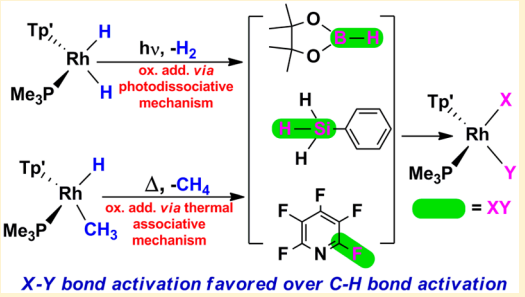

INTRODUCTION

Homogeneous transition metal complexes are now known to activate a wide variety of strong bonds in organic molecules, and selectivities are usually observed when more than one type of bond is present. For example, typical hydrosilylation catalysts activate Si−H bonds in preference to C−H bonds.[1] Similarly, the best borylation catalysts attack B−B and B−H bonds without affecting C−H bonds.[2] While these points may seem hardly worthy of mention, the issue of selectivity becomes critical when we consider C−H functionalization reactions such as the conversion of methane to methanol because suitable methane activators react more rapidly with product than with methane.[3] Carbon−fluorine bond activation is a rarer phenomenon, and the issue of competition between activation of C−F and C−H bonds within the same molecule becomes especially important. Indeed, it is a rarity to discover complexes that activate the C−F bonds of pentafluorobenzene in preference to its C−H bond.[4]

In this paper, we are concerned with two types of competition that occur in oxidative addition reactions involving Si−H, B−H, C−F, and C−H bonds. We refer to reactions with substrates such as alkylsilanes as *intramolecular competition* where reaction can proceed via activation of either C−H or Si−H bonds. We designate reactions with mixtures of two substrates such as benzene and alkylsilanes as *intermolecular competition* reactions. Here, we test the selectivity of one of the most potent C−H activating systems that is very effective for many types of C−H bonds, including those of alkanes.

Metal complexes with tris(pyrazolyl)borate (Tp) ligands have provided several examples of photochemical and thermal C−H bond activation.[5] Of particular interest are the alkane activation reactions of Tp′Rh(CO)$_2$ (Tp′ = tris(3,5-dimethylpyrazolyl)-borate),[6] and the alkene and arene activation reactions of TpIr complexes.[7]

The photochemical activity of Tp′Rh(CNCH$_2$CMe$_3$)(η^2-PhN=C=N-neopentyl) toward a wide variety of hydrocarbon ligands has been investigated.[8] The complex shows kinetic and thermodynamic preference toward primary C−H bonds over secondary C−H bonds of alkanes and aromatic over aliphatic C−H bonds.[9] Studies of kinetic selectivity and reductive elimination rates allowed determination of the energetic barriers for the activation of different C−H bonds.[9,10] Further experiments highlighted a slight preference for the unsaturated fragment [Tp′Rh(CNCH$_2$CMe$_3$)] to coordinate in the first place to

Received: November 4, 2014
Published: December 29, 2014

DOI: 10.1021/ja5113172
J. Am. Chem. Soc. 2015, 137, 1258−1272

secondary C−H bonds to form a σ-alkane complex. The selectivity for C−H oxidative addition of primary C−H bonds was demonstrated to arise through a migration step from a secondary σ-alkane complex to a primary σ-alkane complex followed by C−H oxidative cleavage.[11]

The reactivities of the same photochemical precursor and the thermal precursors Tp′Rh(CNCH$_2$CMe$_3$)(alkyl)H and Tp′Rh(CNCH$_2$CMe$_3$)(Ph)H have been studied in the presence of several different substrates with functional groups: RCl, RCN, RF, CH$_2$F$_2$, Ar^{F}H, ROCH$_3$ (where R = alkyl and Ar^F = C$_6$H$_{5-n}$F$_n$). All show total selectivity for C−H oxidative addition and no cleavage of C−Cl, C−CN, C−F, or C−O bonds.[12,13] The lack of reactivity of alkyl chlorides vs carbon−hydrogen bonds is particularly surprising, considering the widespread reports of R−Cl oxidative addition.[14]

The tris(pyrazolyl)borate rhodium trimethylphosphine dihydride complex Tp′Rh(PMe$_3$)H$_2$ (**1**, Scheme 1) has been investigated less extensively than its carbodiimide analogue but shows similar reactivity.[15,16] It undergoes loss of H$_2$ on photolysis to form the fragment Tp′Rh(PMe$_3$), which also acts as a powerful C−H activator.[17,18] Alternatively, Tp′Rh(PMe$_3$)(CH$_3$)H (**1a**) can act as a thermal precursor of the same fragment.[19] Again C−H activation occurs in preference to C−CN, C−F, and C−O activation. The fragment [Tp′Rh(PMe$_3$)] appeared unreactive toward Et$_3$SiH.[18a] Comparison with the previously studied unsaturated fragments [Cp*Rh(PMe$_3$)] and [Cp*Ir(PMe$_3$)] highlighted similar reactivity toward C−H bonds, suggesting that selectivity is not strongly influenced by the ligand type or the metal center.[13b,20] However, it is established that the weaker C−H bond-activating fragments [CpRh(PPh$_3$)] and [CpRh(PMe$_3$)] activate Si−H and B−H bonds of silanes and alkoxyboranes, respectively, but not the C−H bonds of alkanes.[21] Tests of intermolecular competition show no significant selectivity of the [CpRh(PPh$_3$)] complex between H-Bpin, H-C$_6$F$_5$, and H-SiMe$_2$Et. Tp′Rh(PPh$_3$)$_2$ undergoes thermal Sn−H activation with Ph$_3$SnH and alkyne C−H activation with PhCCH.[22] Intermolecular competition experiments have also been conducted on ruthenium phosphine complexes (see Discussion).[23] Intermolecular competition for oxidative addition may be compared to intramolecular competition for reductive elimination, as the microscopic reverse. In this context, elimination of H-Bpin from CpRhH$_2$(Bpin)(SiR$_3$) was preferred over elimination of H−H or H−SiR$_3$.[24]

Scheme 1. Structures of 1, 1a, and Substrates

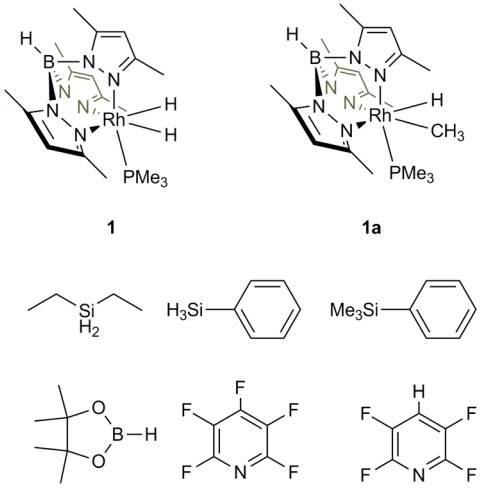

In this paper, we build a detailed picture of the reactivity of **1** and **1a** toward B−H, Si−H, C−F, and C−H bonds. Although [Tp′Rh(PMe$_3$)], derived from **1** or **1a**, is a very strong alkane C−H bond activator, it proves selective toward B−H and Si−H bonds over competing alkyl and aryl C−H bonds in intramolecular competition. Scheme 1 shows the precursor complexes and the substrates. Contrary to expectations, we show that the same species can react by C−F oxidative addition and that C−F bonds are sometimes activated in the presence of competing C−H bonds. We also examine intermolecular competition between activation of the C−H bonds of benzene and the B−H bonds of an alkoxyborane or the Si−H bonds of alkyl/aryl silanes. We show through kinetic studies that the photochemical mechanism of reaction of **1** is markedly different from the thermal mechanism of reaction of **1a**.

RESULTS

The complex Tp′Rh(PMe$_3$)H$_2$ **1** was employed as a photochemical precursor and Tp′Rh(PMe$_3$)(Me)H (**1a**) as a thermal precursor for oxidative addition reactions (Scheme 1). Complex **1** displays a doublet in the ^{31}P{^{1}H} NMR spectrum at δ 3.04 with J_{PRh} = 138 Hz, typical of Rh(III). The ^{1}H NMR spectrum exhibits a hydride resonance at δ −17.09 (dd, J_{RhH} = 21 Hz, J_{PH} = 36 Hz), a doublet for the PMe$_3$ at δ 1.21, four resonances for the CH$_3$ groups of the Tp′ ligand in a 1:2:2:1 ratio, and two signals for the CHs of the Tp′ in a 2:1 ratio at δ 5.52 and 5.77. Complex **1** is pale yellow and exhibits a shoulder at 275 nm (hexane) with a long tail into the visible region in the UV−vis spectrum. Key NMR characteristics of complex **1a** are a ^{31}P{^{1}H} NMR resonance at δ 4.59 (d, J_{RhP} = 148 Hz), together with hydride and methyl resonances in the ^{1}H NMR spectrum at δ −18.14 (dd, J_{RhH} = 24 Hz, J_{PH} = 34 Hz) and 0.98 (d, J_{RhH} = 4 Hz), respectively. Complex **1a** is generated *in situ* in THF and is formed together with some Tp′Rh(PMe$_3$)(trihydrofuranyl)H (**1b**) (6−35%; see Experimental Section).

Reactions of 1 and 1a with HBpin. The irradiation of **1** in neat HBpin (λ > 290 nm, 1 h, room temperature) generates one product cleanly in 90% NMR yield (10% unreacted **1** as determined by ^{31}P{^{1}H} NMR spectroscopy). Removal of HBpin produces a white solid that was fully characterized by multinuclear NMR spectroscopy, liquid injection field desorption/ionization mass spectrometry (LIFDI-MS), and X-ray crystallography. The ^{31}P{^{1}H} NMR spectrum shows a resonance at δ 5.2 (d, J_{RhP} = 145 Hz) (see spectra in Supporting Information). The ^{1}H NMR spectrum reveals a hydride resonance at δ −16.8 (dd, J_{RhH} = 26 Hz, J_{PH} = 31 Hz), and the ^{11}B NMR spectrum shows a broad resonance at δ 39.2 typical of a rhodium boryl species.[2] Finally, the ^{13}C{^{1}H} NMR spectrum reveals the quaternary carbons of the Bpin moiety at δ 81.2, shifted upfield from free HBpin (δ 83.1).[25] We therefore assign the new species as the complex Tp′Rh(PMe$_3$)(Bpin)H (**2**). The thermal reaction of Tp′Rh(PMe$_3$)(CH$_3$)H (**1a**) in the presence of excess HBpin in THF formed **2** quantitatively (in 2 weeks at room temperature or overnight at 40 °C).

The crystal structure confirmed the identity of **2** (Figure 1a, Table 1). The structure is complicated by disorder in the dioxoborolane ring which was modeled with one oxygen occupying two alternative positions in an 88:12 ratio. The Rh−B distance was determined as 2.028(3) Å in agreement with measurements for CpRh(PPh$_3$)(Bpin)H.[21] The hydride in **2** was located in the difference map and, after refinement, found at a distance Rh−H of 1.50(2) Å; the B···H separation was determined as 2.43(2) Å, considerably longer than for CpRh-

DOI: 10.1021/ja5113172
J. Am. Chem. Soc. 2015, 137, 1258−1272

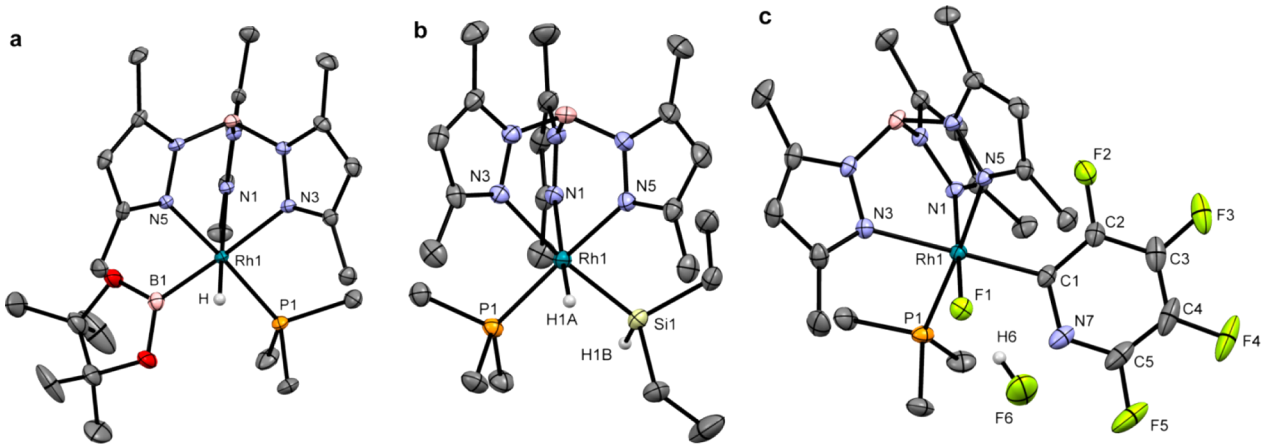

Figure 1. Crystal structures of (a) Tp′Rh(PMe_3)(Bpin)H (**2**) (a second minor disorder component (12%) of the Bpin is not shown), (b) Tp′Rh(PMe_3)(Et_2SiH)H (**3**), and (c) Tp′Rh(PMe_3)(C_5NF_4)(FHF) (**7**). Hydrogen atoms are omitted for clarity apart from those of the bifluoride, hydride, and $SiHEt_2$ ligands. Ellipsoids for the anisotropic displacement parameters at the 50% level.

Table 1. Selected Bond Lengths (Å) and Angles (deg) for Tp′Rh(PMe_3)(Bpin)H (2), Tp′Rh(PMe_3)($SiEt_2H$)H (3), and Tp′Rh(PMe_3)(2-C_5NF_4)(FHF) (7)

2		3		7	
B(1)−Rh(1)	2.028(3)	Si(1)−Rh(1)	2.315(1)	F(1)−Rh(1)	2.0107(12)
H(1)−Rh(1)	1.50(2)	Rh(1)−H(1A)	1.52(3)	C(1)−Rh(1)	2.005(2)
N(1)−Rh(1) trans to H	2.2409(19)	N(1)−Rh(1) trans to H	2.247(2)	N(1)−Rh(1) trans to F	2.0452(17)
N(3)−Rh(1) trans to boryl	2.2966(19)	N(3)−Rh(1) trans to silyl	2.299(3)	N(3)−Rh(1) trans to C_5F_4N	2.1869(17)
N(5)−Rh(1) trans to P	2.1242(18)	N(5)−Rh(1) trans to P	2.124(2)	N(5)−Rh(1) trans to P	2.1138(16)
P(1)−Rh(1)	2.2373(6)	P(1)−Rh(1)	2.2373(8)	P(1)−Rh(1)	2.2927(6)
B(1)···H(1)	2.43(2)	Si(1)···H(1A)	2.62(3)	F(1)···F(6)	2.334(2)
		Si(1)−H(1B)	1.53(3)	F(1)···H(6)	1.41(3)
P(1)−Rh(1)−B(1)	86.78(8)	P(1)−Rh(1)−Si(1)	89.89(3)	P(1)−Rh(1)−F(1)	89.35(4)
B(1)−Rh(1)−H(1)	85.8(9)	Si(1)−Rh(1)−H(1A)	83.4(2)	Rh(1)−F(1)−F(6)	139.28(8)

(PPh_3)(Bpin)H (2.09(2) Å). The B−Rh−H angle of 85.8(9)° is also larger than that determined for the CpRh(PPh_3)(Bpin)H (71.0(8)°). These observations support oxidative addition to form a rhodium-boryl complex rather than η^2-coordination, whereas a residual B···H interaction was suggested[21] for CpRh(PPh_3)(Bpin)H (see also reviews).[26]

The complex Tp′Rh(PMe_3)(Bpin)H (**2**) does not undergo reductive elimination of HBpin even upon heating to 140 °C in benzene or pentafluorobenzene solution. Decomposition was detected at higher temperatures, but no formation of Tp′Rh(PMe_3)(Ph)H or Tp′Rh(PMe_3)(C_6F_5)H was observed.

Reaction of 1 and 1a with Silanes. Complex **1** was irradiated in neat Et_2SiH_2 at room temperature (λ > 290 nm, 9 h), yielding Tp′Rh(PMe_3)($SiEt_2H$)H (**3**) with an NMR yield of 75%, together with minor unidentified products. We observe no products attributable to C−H activation of the ethyl groups. The product exhibits a characteristic hydride resonance at δ −17.9 (dd, J_{RhH} = 21 Hz, J_{PH} = 32 Hz) in the ^{1}H NMR spectrum, and a doublet in the $^{31}P\{^1H\}$ NMR spectrum at δ −0.9 (d, J_{RhP} = 140 Hz). The $\{^1H-^{29}Si\}$ correlation spectrum linked the hydride resonance and the ethyl protons to a ^{29}Si resonance at δ 31.8 (see SI). The remaining Si−H proton resonates at δ 4.36 (br, s).

Crystals of **3** were grown from hexane solution, and the structure was confirmed as Tp′Rh(PMe_3)($SiEt_2H$)H (Figure 1b, Table 1). The Rh−Si bond length was found to be 2.315(2) Å. The hydride and the hydrogen atom bound to the Si atom were located in the difference map. The Rh−H1A bond length was determined as 1.52(3) Å and the Si···H1A distance as 2.62(3) Å; this value is considerably larger than what is expected for secondary interactions between Si and H (SISHA),[27] confirming that complete oxidative addition occurred. The values for the P−Rh−H and Si−Rh−H angles also indicate that no residual Si···H interaction is present.[21]

The complex Tp′Rh(PMe_3)($SiEt_2H$)H (**3**) does not undergo reductive elimination of Et_2SiH_2 upon heating to 130 °C in benzene or pentafluorobenzene solution. Decomposition of **3** was observed above this temperature.

Photolysis of **1** in neat $PhSiH_3$ (λ > 290 nm, 5 h, room temperature) leads to production of Tp′Rh(PMe_3)($SiPhH_2$)H (**4**) in 80% NMR yield. The hydride appears at δ −16.7 (dd, J_{RhH} = 20 Hz, J_{PH} = 31 Hz). The SiH_2 group is diastereotopic, exhibiting resonances at δ 4.98 (dd) and 5.28 (m). The $^{31}P\{^1H\}$ spectrum shows a doublet at δ 1.9 (J_{RhP} = 131 Hz) and a broad ^{29}Si NMR resonance at δ −15.8. The remaining 20% is shared between three other hydride products, which all have $J_{PH} \approx 30$ Hz, $J_{RhH} \approx 25$ Hz, and $J_{RhP} \approx 145$ Hz, with hydride chemical shifts close to δ −17. They are assigned to the three isomers (*ortho*, *meta*, *para*) of Tp′Rh(PMe_3)($C_6H_4SiH_3$)H (**4a**) on the basis of their similarity to the resonances of Tp′Rh(PMe_3)(C_6H_5)H and those of the product derived from reaction with $PhSiMe_3$ described below (Table 2). Parent ions were observed for both **3** and **4** by LIFDI-MS.

A solution of complex **1** in neat $PhSiMe_3$ was photolyzed (λ > 290 nm, 7 h, room temperature) in order to compare to the additional products observed in the reaction with $PhSiH_3$. The three products detected after short photolysis time (50% NMR conversion) by $^{31}P\{^1H\}$ NMR spectroscopy showed $J_{RhP} \approx 146$

DOI: 10.1021/ja5113172
J. Am. Chem. Soc. 2015, 137, 1258−1272

Table 2. Principal NMR Parameters for Products Formed by Aromatic C−H Bond Activation

substrate[a]	product	δ (^{1}H)	J_{RhH}, Hz	δ (^{31}P)	J_{RhP}, Hz
$PhSiH_3$	**4a** (three isomers)	−16.80	25.0	2.5	145.7
		−16.82	24.9	2.0	145.2
		−16.90	25.3	1.9	145.2
$PhSiMe_3$	**5** (three isomers)	−16.86	25.0	2.8	146.5
		−16.87	24.7	3.1	146.3
		−16.91	25.2	2.7	145.7
C_6H_6	Tp′Rh(PMe_3)(Ph)H	−16.90	25.4	1.6	146.0

[a] C_6D_6 solvent. Spectra run at 500 MHz and room temperature.

Hz. Three hydride resonances appeared in the ^{1}H NMR spectrum, with J_{PH} and J_{RhH} measured to be very similar to the ones determined for the hydrides observed in the reaction with $PhSiH_3$ (Table 2). All these resonances were linked to the doublets observed in the ^{31}P{^{1}H} spectrum by ^{31}P−^{1}H HMQC spectroscopy and assigned as the *ortho*, *meta*, and *para* isomers of Tp′Rh(PMe_3)($C_6H_4SiMe_3$)H (**5**).

The reaction of **1a** was also carried out with each of Et_2SiH_2, $PhSiH_3$, and $PhSiMe_3$. Complete conversion with Et_2SiH_2 and $PhSiH_3$ was achieved at room temperature to form the complexes **3** and **4** + **4a** in 9 days and 1 day, respectively. For comparison, reaction of **1a** with C_6H_6 at room temperature gives complete conversion to Tp′Rh(PMe_3)(Ph)H in ca. 10 h (three half-lives). The thermal route toward the formation of the complexes **2**, **3**, and **4**, although slower than the photoconversion, was more selective and facilitated the access to analytically pure material. Activation of $PhSiMe_3$ with **1a** gave three sets of doublets in the ^{31}P{^{1}H} NMR spectrum as well as overlapped hydride signals in the ^{1}H NMR spectrum after 20 h at room temperature, consistent with the products from photolysis of **1** with $PhSiMe_3$ and are assigned to the three isomers of **5**.

Reaction of 1 and 1a with C_5NF_5 and C_6F_6. The irradiation of **1** in neat pentafluoropyridine (λ > 290 nm, 5 h, room temperature) cleanly generates one product as a mixture of two isomers (>80% conversion). Removal of solvent gives a colorless solid that was redissolved in C_6D_6 and characterized by multinuclear NMR spectroscopy. The ^{31}P{^{1}H} NMR spectrum shows a resonance at δ 6.67 (dd, J_{RhP} = 129 Hz, J_{PF} = 17 Hz) for the major isomer. The value of J_{RhP} indicates a Rh(III) oxidation state,[28] and the values of J_{FP} are similar to those for Cp*Rh(PMe_3)(C_6F_5)F.[29] A broad resonance was found in the metal-fluoride region of the ^{19}F NMR spectrum at δ −428.8, consistent with a Rh−F bond. Low-temperature ^{19}F NMR spectroscopy sharpened the resonance, enabling J_{RhF} to be measured as 182 Hz. The product was assigned as the Tp′Rh(PMe_3)(2-C_5NF_4)F complex **6**.

The minor isomer exhibited very similar spectra to the major isomer. The two species were assigned as two rotamers in a 10:1 ratio, both with C−F activation at the position *ortho* to nitrogen. In the ^{19}F NMR spectrum, each of the fluoroaromatic resonances of the major isomer had a partner adjacent to it for the minor isomer (δ −85.9/−84.6; −133.0/−129.9; −148.3/−146.6; −169.0/−168.5). Prior studies of polyfluoroaryl derivatives of the type Tp′Rh(PMe_3)(aryl^F)H showed hindered rotation around the Rh−aryl^F bond, resulting in observable rotamers.[18a] Only two of the fluorine resonances, of unequal intensities, were in the region for F adjacent to N (δ −85.9/−84.6). The observation of unequal intensity is inconsistent with formation of the *meta* or *para* isomer or mixtures of *meta* and *para* isomers. The ^{19}F resonance of the second isomer in the high field region was detected at low temperature as a weak and broad resonance at δ −455.4 (see SI). The chirality at rhodium was demonstrated by the appearance of three singlets for the Tp′-methine groups and six resonances for the inequivalent Tp′-methyls. On scaling up the reaction, crystals were obtained from a hexane solution which were determined by X-ray structural analysis to be the *bifluoride* analogue Tp′Rh(PMe_3)(2-C_5NF_4)(FHF) (**7**), where a molecule of HF is coordinated to the fluoride atom (Figure 1c). The thermal reaction of **1a** with pentafluoropyridine was also investigated and yielded **6** as the major product together with some minor byproducts, but **7** was not observed. The reaction was complete after 2 days at room temperature.

NMR spectroscopic characterization of the bifluoride complex Tp′Rh(PMe_3)(C_5NF_4)(FHF) (**7**) revealed the typical features for this class of complex. A broad low-field resonance (δ 10.7, F*H*F) in the ^{1}H NMR spectrum appears as a doublet (J_{HF} = 447 Hz) at 205 K in toluene, which can be associated with coupling to the distal fluorine of a FHF ligand. The ^{31}P{^{1}H} NMR spectrum shows a doublet of doublets at δ 6.70 with very similar coupling constants to those observed for the fluoride analogue. The ^{19}F NMR spectrum at 205 K shows resonances at δ −398.9 assigned to the proximal fluorine (directly bonded to Rh), and at δ −178.7 (J_{FH} = 447 Hz) assigned to the distal fluorine (see SI). Complex **7** is detected as a single rotamer. All the NMR data for the bifluoride complex **7** are consistent with observations for Ru(diphosphine)$_2$(FHF)H and Rh(NHC)(PPh_3)$_2$(FHF) complexes.[30]

The crystal structure of **7** (Figure 1c, Table 1) shows the presence of the bifluoride, FHF, coordinated to the rhodium; the acidic proton was not found by Fourier difference map and was located by taking into account the known HF bond distance.[31] The Rh−F bond length (2.0107(12) Å) is closer to the value for Rh(COD)(PPh_3)F (2.0214(12) Å) than that in Rh(COD)(PPh_3)(FHF) (2.083(2) Å).[32] The short Rh−F bond probably reflects very weak RhF···HF hydrogen bonding. The Rh−F···F angle and F(1)···F(6) distance in **7** are similar to those reported for *trans*-[Rh(Ph_3P)$_2$(Ph_2PF)(FHF)].[33] The fluoride complex **6** acted as a trap for HF, as shown by the isolation of **7**. In spite of much effort, we have not identified the source of HF. The weakness of the hydrogen bond is further confirmed by the observation that bifluoride **7** reverts to fluoride **6** when the complex is left in solution for a few days. This can be understood by HF attack on the glass NMR tube.[34a,b] Irradiation of **1** in hexafluorobenzene (99.5%) resulted in slow loss of **1**, but no formation of metal fluoride complexes or Tp′Rh(PMe_3)(η^2-C_6F_6). Instead, the [Tp′Rh(PMe_3)] fragment scavenged impurities in the C_6F_6, yielding a variety of products, among which we identified Tp′Rh(PMe_3)(C_6F_5)H[18a] and Tp′Rh(PMe_3)(H)Cl (^{1}H δ −17.30, dd, J_{RhH} = 12 Hz, J_{PH} = 28 Hz; ^{31}P{^{1}H} δ 1.3, d, J_{RhP} = 122 Hz). Since C_6F_6 appeared to be unreactive, we selected it as a solvent for our kinetic investigations.

DOI: 10.1021/ja5113172
J. Am. Chem. Soc. 2015, 137, 1258−1272

Scheme 2. Photochemical Reactivity of Tp′Rh(PMe$_3$)H$_2$ (1) and Thermal Reactions of Tp′Rh(PMe$_3$)(CH$_3$)H (1a)[a]

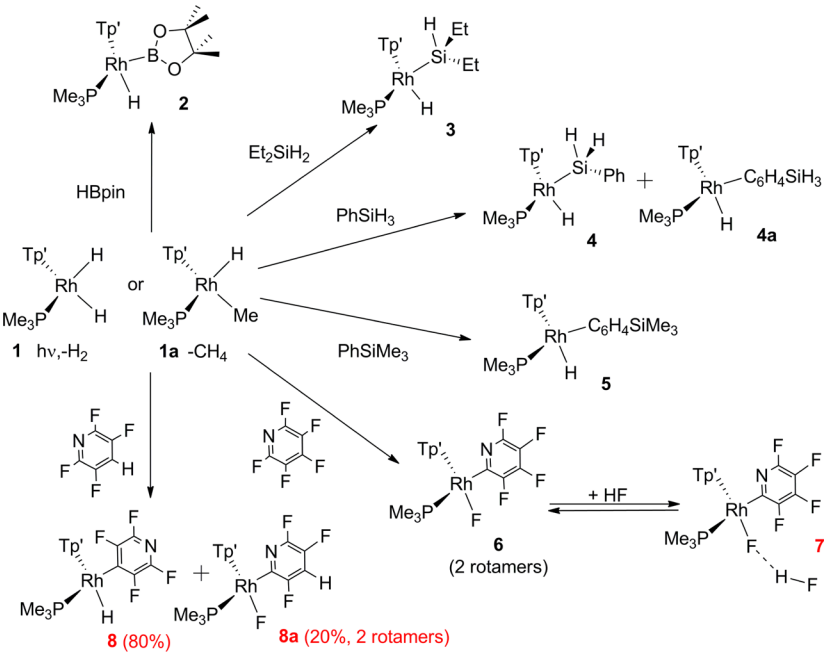

[a]The products **7**, **8**, and **8a** were only investigated photochemically and are shown in red.

Photoreaction of 1 with 2,3,5,6-Tetrafluoropyridine. The photochemical reaction of **1** in neat 2,3,5,6-tetrafluoropyridine was investigated in order to explore intramolecular competition between C−H and C−F activation. After photolysis (5 h) the reaction reached 30% conversion; the solvent was removed under vacuum and the solid redissolved in C_6D_6. The $^{31}P\{^1H\}$ NMR spectrum showed the appearance of two new products in 4:1 ratio at δ −2.3 (dd, J_{RhP} = 127 Hz, J_{PF} = 20 Hz) and 4.6 (dd, J_{RhP} = 132 Hz, J_{PF} = 18 Hz), respectively, suggesting coupling to ^{103}Rh and to ^{19}F (see SI). The ^{1}H NMR spectrum of the major product revealed a new hydride resonance at δ −15.5 (ddd, J_{PH} = 25 Hz, J_{FH} = 19 Hz, J_{RhH} = 14 Hz), which was coupled to the $^{31}P\{^1H\}$ resonance at δ −2.3, as indicated by $\{^1H-^{31}P\}$ HMQC spectroscopy. This species was assigned as Tp′Rh(PMe$_3$)(4-C$_5$NF$_4$)H (**8**). The ^{19}F NMR spectrum shows a characteristic rhodium-fluoride peak at δ −430.1 for the minor product (d, J_{FRh} = 181 Hz). Other ^{19}F resonances for the two fluoropyridyl groups of **8** and **8a** can also be identified. On the basis of these results, we assigned the minor product to the C−F activated complex Tp′Rh(PMe$_3$)(2-C$_5$NF$_3$H)F (**8a**); in addition, a minor rotamer of Tp′Rh(PMe$_3$)(2-C$_5$NF$_3$H)F is detected by $^{31}P-^1H$ HMQC and by ^{19}F NMR spectroscopy, ca. 5%. The aromatic proton in the minor product was detected at δ 6.2. The 4:1 ratio for **8** and **8a** shows that C−H activation is favored, but to our surprise C−F activation also took place. This observation contrasts with the previous results on reactivity of **1** toward fluorinated arenes, where C−H activation was observed exclusively.[13a,18a] A brief investigation of the photochemical reaction of **1** with 2,6-difluoropyridine generated full conversion to two isomers of Tp′Rh(PMe$_3$)(C$_5$NH$_2$F$_2$)H with no evidence for C−F bond activation.[35]

Overall Reactivity. The complete set of photochemical reactions of **1** and thermal reactions of **1a** are summarized in Scheme 2.

Photochemical Kinetic Experiments. *Concentration Dependence.* The kinetics for the reaction of **1** with HBpin and $PhSiH_3$ were investigated to obtain additional information about the mechanism. Solutions of **1** in C_6F_6 as a solvent in the presence of different concentrations of HBpin or $PhSiH_3$ were monitored either by $^{31}P\{^1H\}$ inverse gated or by $^1H\{^{31}P\}$ NMR spectroscopy at different photolysis times (λ > 290 nm) (see SI). The spectra were measured at low conversion to avoid the effects of secondary photolysis. Formation of some Tp′Rh(PMe$_3$)(H)Cl (ca. 3%) from reaction of **1** with impurities in the solvent C_6F_6 was detected for both of the reactions and was accounted for in the kinetic analysis. The relative areas obtained from the integration of the hydride peaks for **2** and **4** proved to be essentially independent of the substrate concentration (0.2−2 M) (Figure 2).

The experimental data are consistent with a dissociative pathway where the first photochemical step is H_2 photodissociation and the back reaction with H_2 is slow compared to

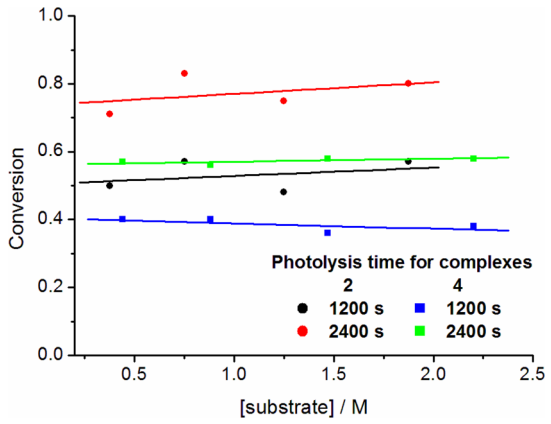

Figure 2. Effect of [substrate] on the photochemical conversion of **1** to product for two different photolysis times. Circles: conversion of **1** to **2**, squares: conversion of **1** to **4**, where conversion = $I_{PRODUCT}/(I_{PRODUCT} + I_{PRECURSOR} + I_{BYPRODUCT})$.

DOI: 10.1021/ja5113172
J. Am. Chem. Soc. 2015, 137, 1258−1272

the reaction of the photogenerated unsaturated 16e$^-$ fragment [Tp′Rh(PMe$_3$)] with the substrate. The alternative mechanism of photochemical de-coordination of one arm of the Tp′ ligand, followed by reaction with substrate, should yield second-order kinetics (or saturation kinetics), since the intramolecular back reaction should be much faster than the reaction with substrate.[6d,36]

In Situ Photolysis Studies at 355 nm. The photochemical kinetics were studied further by irradiating *in situ* within the NMR probe with a monochromatic laser source at 355 nm using C_6F_6 as a solvent. UV/vis spectra measured at this wavelength show that the absorbance of the substrate and that of the solvent are both less than that of **1**. A dilute solution of **1** was prepared (ca. 6 mM) with absorbance of ca. 0.5 in a 5 mm path length (the molar absorption coefficient is 180 M^{-1} cm^{-1} at 355 nm) and a concentration of $PhSiH_3$ of ca. 0.4 M. The photochemical reaction was followed *in situ* by $^1H\{^{31}P\}$ NMR spectroscopy at room temperature. The decay of **1** and the growth of **4** were linear with respect to time (Figure 3), consistent with the dissociative kinetic model where the rate of change of concentration is only dependent on light absorbed.

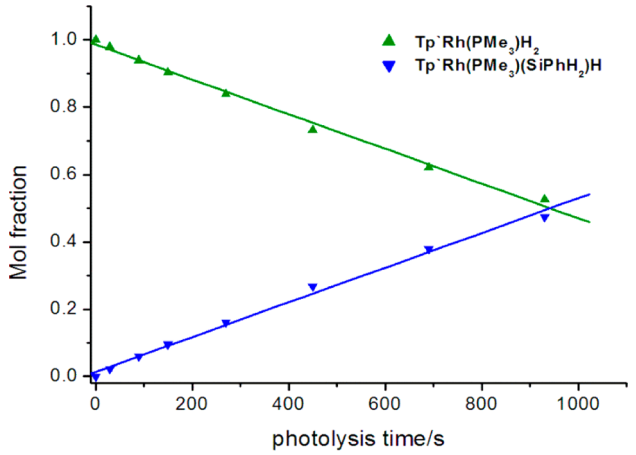

Figure 3. Conversion of **1** to **4** as a function of monochromatic photolysis time.

Competition Reactions with *in Situ* Photolysis. In order to investigate the selectivity of complex **1** for the activation of B−H, Si−H, and C−F bonds compared to benzene C−H bonds, we conducted photochemical experiments with monochromatic light in the presence of both the substrate and benzene in C_6F_6 solution. The samples were irradiated *in situ* as above, and $^1H\{^{31}P\}$ NMR spectra were acquired as a function of time, following the reaction with HBpin and $PhSiH_3$ by the evolution of the hydride peaks with [benzene] = [substrate] = 0.5 M. The competition reaction with C_5NF_5 was conducted instead with 1:3 benzene/pentafluoropyridine (0.5 and 1.5 M, respectively) in C_6F_6 in order to push the reaction toward activation of the C−F bond and was followed by monitoring the PMe_3 resonances in the $^1H\{^{31}P\}$ NMR spectra. Product ratios were determined up to ~50% since secondary photolysis of the products is significant.[37] The experimental points were fitted to a linear regression (Figure 4) and the gradients used as relative rate constants to determine the selectivity (Table 3).[38] The mechanistic implications are analyzed in the Discussion.

Thermal equilibration of the final products was excluded considering that the complexes were found to be stable in benzene solution at temperatures up to 140 °C. Photochemical equilibration was also explored; since the reactions were taken to relatively small conversion and the product distribution varied only slightly during this period, we conclude that photochemical equilibration did not play any role in the product ratio.[37]

All of the data from the photochemical experiments point to a dissociative mechanism in which H_2 is reductively eliminated

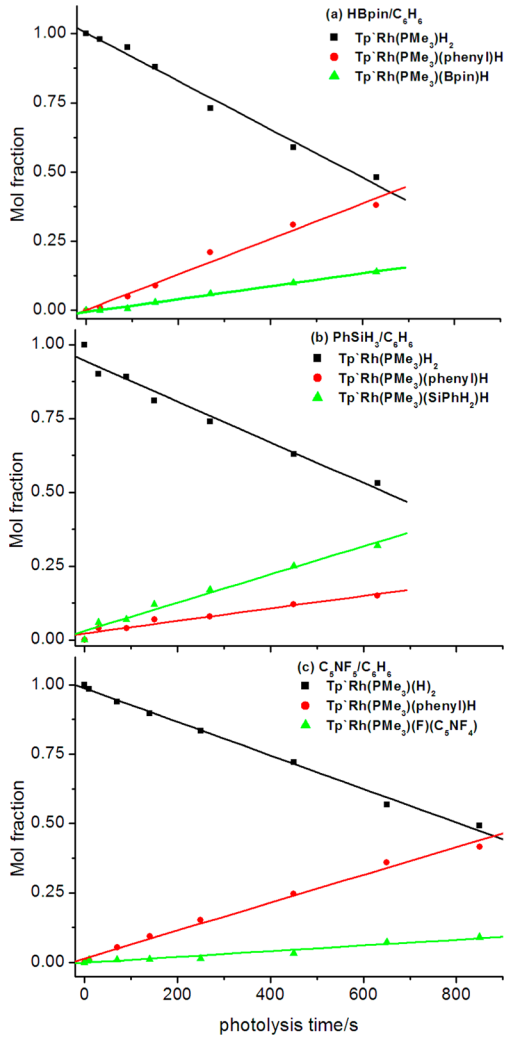

Figure 4. Product distribution of photochemical competition reactions of **1** with the investigated substrates and C_6H_6 as competing ligand: (a) HBpin/C_6H_6, (b) $PhSiH_3/C_6H_6$, and (c) C_5NF_5/C_6H_6. Gradients are given in the Supporting Information.

Table 3. Results of Photochemical Competition Reactions[a]

substrate (X)	mole ratio [X]/[C_6H_6]	intermolecular selectivity,[b] $k_X/k_{C_6H_6}$
C_5NF_5	3	0.068 ± 0.003[c]
HBpin	1	0.364 ± 0.008
$PhSiH_3$	1	2.3 ± 0.1
substrate		intramolecular selectivity
HBpin		>50 in favor of BH
Et_2SiH_2		>50 in favor of SiH
$PhSiH_3$		4.0 ± 0.2 in favor of SiH
C_5NF_4H		4.0 ± 0.2 in favor of CH

[a]Measured in C_6F_6 solution with 355 nm radiation, by integration of $^1H\{^{31}P\}$ resonance. [b]Error bars given as standard deviations derived from linear regression. [c]Observed product ratio has been corrected for relative concentration of substrates.

DOI: 10.1021/ja5113172
J. Am. Chem. Soc. 2015, 137, 1258−1272

from the excited state leading to [Tp′Rh(PMe$_3$)] as an intermediate, which undergoes reaction with the different substrates in its ground electronic state as in eq 1 (see also Discussion and Conclusions).

$$\mathrm{Tp'Rh(PMe_3)H_2} \overset{h\nu}{\rightleftarrows} [\mathrm{Tp'Rh(PMe_3)H_2}]^* \xrightarrow{-\mathrm{H_2}} [\mathrm{Tp'Rh(PMe_3)}] \xrightarrow{+\mathrm{XY}} \mathrm{Tp'Rh(PMe_3)(X)Y} \quad (1)$$

The kinetic experiments are carried out with monochromatic 355 nm radiation in a region where **1** is the major light absorber. They show kinetics that are zero-order in [substrate], indicating that the quantum yield should also be independent of substrate. The preparative experiments described earlier were carried out with white light with $\lambda > 300$ nm and with the substrate as solvent. The variations in photolysis time required in these experiments may be attributed to differences in absorption by the solvent and changes in quantum yield with solvent.[38]

Scheme 3. Kinetic Analysis of Reactivity of 1a

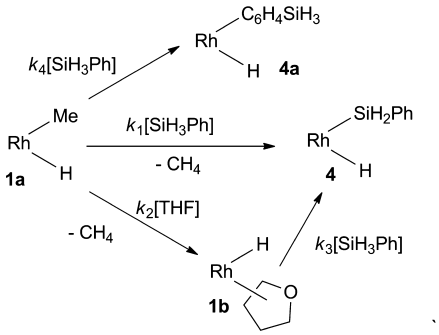

Thermal Kinetic Studies of PhSiH$_3$ Activation. The kinetics of the reaction of Tp′Rh(PMe$_3$)(CH$_3$)H (**1a**) with PhSiH$_3$ were studied by ^{31}P{^{1}H} NMR spectroscopy. The preparation of **1a** also produces some Tp′Rh(PMe$_3$)-(trihydrofuranyl)H (**1b**, 2- and 3-isomers) during the isolation of the material from the THF solution in which it is prepared. As earlier studies of benzene activation by the related species Tp′Rh(CNneopentyl)(CH$_3$)H showed evidence for an associative mechanism, reaction of **1a** with PhSiH$_3$ was anticipated to also be associative.[39] Reactions of this mixture of **1a** and **1b** with PhSiH$_3$ were therefore examined at different concentrations of silane in THF, and the distribution of species was simulated using the reactions shown in Scheme 3. Here, reaction of **1a** with PhSiH$_3$ in THF solution could produce Si−H activation product **4**, THF activation product **1b**, or aryl C−H activation products **4a**. These reactions all proceed under pseudo-first-order conditions with observed rate constants k_{obs1}, k_{obs2}, and k_{obs4} corresponding to k_1[PhSiH$_3$], k_2[THF], and k_4[PhSiH$_3$], respectively. Complex **1b** can then also react with PhSiH$_3$ to give **4** with a rate constant k_{obs3}, expected to correspond to k_3[PhSiH$_3$].

First, rate constant k_{obs2} ($=k_2$[THF]) was determined by monitoring the conversion of **1a** to **1b** in neat THF at 21 °C, giving $k_{obs2} = (4.72 \pm 0.10) \times 10^{-3}$ min^{-1}, which corresponds to $k_2 = (3.83 \pm 0.08) \times 10^{-4}$ M^{-1} min^{-1}. Second, **1a** (containing ~25% **1b** also) was reacted with neat PhSiH$_3$ to produce **4** and **4a** (4.8:1). Kinetic simulation of these reactions according to Scheme 3 produced initial second-order rate constant values for k_1, k_3, and k_4. Third, reactions were run with solutions of PhSiH$_3$ in THF with varying concentration, which again showed conversion of **1a** and **1b** to **4** and **4a**. The rates of product formation clearly varied with [PhSiH$_3$]; to quantify this, each run was simulated, and the values for k_{obs1}, k_{obs3}, and k_{obs4} were optimized. Table 4 shows the concentrations of PhSiH$_3$ and THF employed and the pseudo-first-order rate constants that were obtained.

These pseudo-first-order rate constants were then plotted vs [PhSiH$_3$] (for k_{obs1}, k_{obs3}, and k_{obs4}) or [THF] (for k_{obs2}). As Figure 5 shows, linear relationships are seen with negligible intercepts for the reactions involving **1a**, indicating a pure second-order reaction with PhSiH$_3$ or THF. The reaction of the trihydrofuranyl hydride **1b**, however, has a clear first-order component ($k_3' = (7 \pm 1) \times 10^{-3}$ min^{-1}) as indicated by the nonzero intercept, as well as a second-order component ($k_3 = (0.73 \pm 0.07) \times 10^{-3}$ M^{-1} min^{-1}). The values of the slopes (second-order rate constants) and intercepts (first-order rate constants) are indicated in Table 5. These variable concentration experiments show that the activation of PhSiH$_3$ proceeds via a

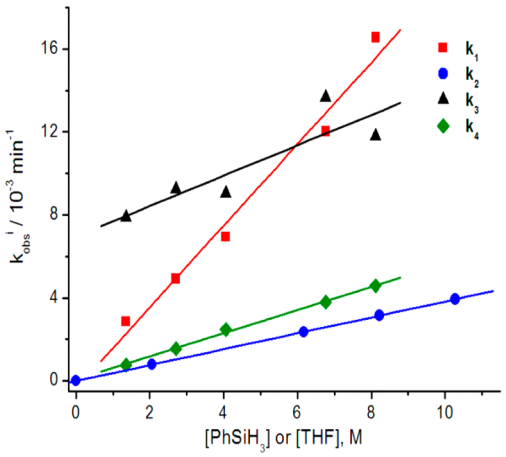

Figure 5. Plots of pseudo-first-order rate constant vs [PhSiH$_3$] or [THF] for the reactions in Scheme 3.

Table 4. Optimized Pseudo-First-Order Rate Constants for Reactions of 1a and 1b with PhSiH$_3$ and THF at 21 °C[a,b]

run	[PhSiH$_3$], M	[THF], M	k_{obs1}, 10^{-3} min^{-1}	k_{obs2}, 10^{-3} min^{-1}	k_{obs3}, 10^{-3} min^{-1}	k_{obs4}, 10^{-3} min^{-1}
1	0	12.33	0	4.7 ± 0.1	0	0
2	1.35	10.28	2.9 ± 0.2	3.93 ± 0.08	7.8 ± 0.2	0.77 ± 0.01
3	2.70	8.22	4.9 ± 0.3	3.15 ± 0.07	9.2 ± 0.4	1.5 ± 0.2
4	4.06	6.17	7.0 ± 0.4	2.36 ± 0.05	9.1 ± 0.3	2.5 ± 0.2
5	6.76	2.06	12.0 ± 0.7	0.79 ± 0.02	14 ± 1	3.8 ± 0.4
6	8.11	0	16.6 ± 0.4	0	12 ± 2	4.6 ± 0.2

[a]All simulations conducted with $k_2 = (3.83 \pm 0.08) \times 10^{-4}$ M^{-1} min^{-1} and $k_{obs2} = k_2$[THF]. [b]Error bars are given as standard deviations derived from linear regression.

DOI: 10.1021/ja5113172
J. Am. Chem. Soc. 2015, 137, 1258−1272

Table 5. Optimized Second-Order and First-Order Rate Constants for Reaction of 1a and 1b with $PhSiH_3$ and THF at 21 °C[a]

reaction step	2nd-order k_i, 10^{-3} M^{-1} min^{-1}	1st-order k_i', 10^{-3} min^{-1}
k_1	2.0 ± 0.2	
k_2	0.383 ± 0.001	
k_3	0.73 ± 0.07	7 ± 1
k_4	0.56 ± 0.02	

[a]Error bars are given as standard deviations on linear regression.

bimolecular pathway from **1a**, but via a predominantly unimolecular pathway (~90% @ 1 M $PhSiH_3$) commencing from **1b**. This result can be interpreted in terms of **1a** forming a σ-CH_4 complex with concomitant conversion from κ^3-Tp′ to κ^2-Tp′; this intermediate undergoes a bimolecular reaction with the substrate ($PhSiH_3$ or THF) to give products **4**, **4a**, or **1b** (Scheme 4). The reactivity of **1b** is understood in terms of a dissociative elimination of THF from **1b** in competition with a displacement of the THF by substrate in a σ-C−H complex of THF.

Scheme 4. Mechanism of Reaction of 1a

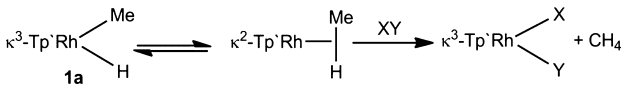

Thermal Competition Reactions with 1a. Competition reactions for **1a** were conducted with mixtures of benzene and $PhSiH_3$ and mixtures of benzene and $PhSiMe_3$. Product distributions were monitored by $^{31}P\{^1H\}$ NMR spectroscopy with inverse gated decoupling. Reaction of **1a** with equal volumes of $PhSiH_3$ and C_6H_6 (without THF) generated a mixture of **4** and $Tp'Rh(PMe_3)(Ph)H$ in a ratio of 1:0.29 after 30 min (24% completion). At higher conversion, the ratios were little changed. Given the mole ratio of $PhSiH_3$ and C_6H_6 (1:1.47), the value of k_{SiH}/k_{PhH} is 5.1 in favor of Si−H activation.

Similar competition reactions were performed with dilute solutions of **1a**, $PhSiH_3$, and C_6H_6 in THF. The first reaction (1.01 M $PhSiH_3$, 1.40 M benzene in THF) was complete after 1 day to give **4** in 94% yield by NMR. The second reaction was run under more dilute conditions (0.14 M $PhSiH_3$, 0.19 M benzene in THF) and reached 76% completion after 1 day with **4** as 93% of the product. Thus, there was an almost exclusive preference for Si−H activation over C−H activation in dilute solutions.

The intermolecular selectivity for $PhSiMe_3$ compared to benzene was determined by dissolving **1a** in a mixture with equal volumes of $PhSiMe_3$ and benzene (mole ratio 0.52 $PhSiMe_3$: 1 benzene). All the three isomers of **5** were seen and their combined integrals were used to give a product ratio of 0.3 from which we deduce that $k(PhSiMe_3)/k(benzene) = 0.58$.

Calculated Energetics of Reactions. The intramolecular selectivity and the lack of reductive elimination of the boryl and silyl complexes, **2**, **3**, and **4** led us to the hypothesis that these complexes may be thermodynamically stable with respect to reductive elimination and reaction with benzene. We therefore undertook calculations of the energetics of the corresponding reactions by DFT methods as in eq 2, using the full structures in all the calculations (see Computational Methods).

$$Tp'Rh(PMe_3)(E)H + C_6H_6 \rightarrow Tp'Rh(PMe_3)(C_6H_5)H + EH \quad (E = Bpin,\ SiH_2Ph,\ SiHEt_2) \qquad (2)$$

The results demonstrate decisively that these reactions have positive free energies when the ligand is coordinated through boron or silicon (Table 6). We also considered the products of

Table 6. Calculated Energies of Reactions in Eqs 2 and 3 (kcal/mol)[a] at 298 K

	ΔH(gas)	ΔG(gas)	ΔG(PCM), C_6H_6
Reactions as for Eq 2			
$Tp'Rh(PMe_3)(Ph)H$	0.0	0.0	0.0
$Tp'Rh(PMe_3)(C_6F_5)H$	12.4	12.2	8.0
$Tp'Rh(PMe_3)(Me)H$	−7.1	−5.5	−9.5
$Tp'Rh(PMe_3)(Bpin)H$	12.9	13.2	9.0
$Tp'Rh(PMe_3)(SiEt_2H)H$	9.6	9.0	6.5
$Tp'Rh(PMe_3)(SiPhH_2)H$	16.0	15.5	13.6
Reactions as for Eq 3			
$Tp'Rh(PMe_3)(4\text{-}C_6H_4SiH_3)H$	1.2	1.2	−4.2
$Tp'Rh(PMe_3)(CH_2R)H$ from HBpin	−23.2	−23.4	−28.2
$Tp'Rh(PMe_3)(CH_2CH_2SiEtH_2)H$	−8.4	−8.7	−12.5

[a]The B3LYP functional was employed.

C−H oxidative addition of the substrates, such as $Tp'Rh(PMe_3)(C_6H_4SiH_3)H$. The reactions of these carbon-coordinated species with benzene (eq 3) were all calculated to have negative free energies. (In order to locate a minimum of the C−H activated HBpin, we restrained the B−H bond length; otherwise it converged on the B−H activated product.)

$$Tp'Rh(PMe_3)(E)H + C_6H_6 \rightarrow Tp'Rh(PMe_3)(C_6H_5)H + EH \quad (E = Bpin,\ SiH_2Ph,\ SiHEt_2) \qquad (3)$$

with

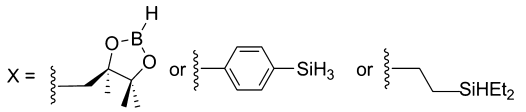

We conclude that reaction of $[Tp'Rh(PMe_3)]$ at the B−H or Si−H bond of HBpin, $PhSiH_3$, and Et_2SiH_2 is energetically preferred to reaction at the C−H bonds of these substrates. Moreover, the reaction products are observed to be stable with respect to reaction with benzene as in eq 2. According to the calculations, the free energies of eq 2 follow the order E = SiH_2Ph > Bpin > $SiHEt_2$.

The bond energies for the substrates (H−E) and the complexes (Rh−E) were also calculated (Table 7). The H−E bonds of H−Bpin and the silanes are weaker than those of the hydrocarbons, but the Rh−B bond is stronger than the Rh−Ph bond and the Rh−Si bonds have essentially the same energy as the Rh−Ph bond. The difference in bond energy between H−Ph and Rh−Ph is 41.9 kcal/mol (37% of the H−Ph energy). A similar difference is found between H−H and H−Rh, whereas the corresponding differences for the remaining substrates are in the range 23−30 kcal/mol (25−29%). As a consequence, the free energy for reductive elimination of H−E and oxidative addition of benzene is unfavorable (eq 2). The free energy for reductive elimination of H−E and oxidative addition of H−C_6F_5 is predicted to be slightly favorable for H−$SiEt_2H$, but unfavorable for the others. Indeed, we observe no reaction between the Rh−B or Rh−Si compounds with benzene or C_6F_5H. The experimental values for H−$SiMe_2H$ and H−$SiPhH_2$ are 93.5 ± 1.2 and 91.3 ±

DOI: 10.1021/ja5113172
J. Am. Chem. Soc. 2015, 137, 1258−1272

Table 7. Calculated Bond Energies for Tp′Rh(PMe$_3$)(E)H (kcal/mol)[a]

E	BDE(H−E)	BDE(Rh−E)	difference BDE(H−E) − BDE(Rh−E)[b]
−H	103.5	67.6	35.9 (35%)
−C$_6$H$_5$	112.3	70.0	41.9 (37%)
−C$_6$F$_5$	118.8	89.2	29.6 (24.9%)
−Bpin	108.6	81.1	27.5 (25.3%)
−SiEt$_2$H	94.8	67.2	27.6 (29.1%)
−SiPhH$_2$	91.7	68.0	23.7 (25.8%)

[a]The M06-2X functional was used. [b]The difference is given in kcal/mol and as a percentage of BDE(H−E).

1.2 kcal/mol, respectively, within 1.3 kcal/mol of the calculated values.[40] We have found no experimental B−H bond energies that match the H−B(OR)$_2$ motif. There is little experimental data on metal-silyl bond energies for comparison but one important result is D(Pt−Si) for the complex [PtIMe$_2$(Me$_3$Si)-(bpy)] is 55.7 ± 3.3 kcal/mol, 24 kcal/mol larger than experimentally determined values for Pt(IV)−CH$_3$ bond energies.[41] Another study on Pt(II) complexes established the sum of the Pt−Si and Pt−H bond energies as 104 kcal/mol for *cis*-Pt(PCy$_3$)$_2$(SiPh$_3$)H.[42] Experimental values of metal−boryl bond energies are equally scarce. The sum of the Ir−B and Ir−H bond energies in *trans*-[Ir(CO)(PPh$_3$)$_2$(Cl)(H)(Bcat)] has been measured as 126.4 kcal/mol, and an estimate of the Ir−B energy has been derived from this as 66 kcal/mol, compared with 35 kcal/mol for the Ir−CH$_3$ bond in *trans*-[Ir(CO)(PPh$_3$)$_2$(Cl)-(Me)(I)].[43] Our calculated values for (D(Rh−H) + D(Rh−Si)) and (D(Rh−H) + D(Rh−B) are 136 and 149 kcal/mol, respectively. Calculated bond energies Ru(PH$_3$)(CO)(Cl)(X) have been compared for X = SiMe$_3$, H and BOCH$_2$CH$_2$O and followed the trend Ru−B (70.9 kcal/mol) > Ru−H (67.2 kcal/mol) > Ru−Si (51.4 kcal/mol). Notably, the bond energies to carbon followed the same trend: C−B > C−H > C−Si.[44]

The photochemical reaction with pentafluoropyridine yields the product of C−F activation at the 2-position, **6**. We undertook DFT calculations to establish the relative stability of the possible isomers, yielding relative free energies after solvent correction as follows: 2-C$_5$NF$_4$, 9.2 kcal/mol; 3-C$_5$NF$_4$, 0.01 kcal/mol; and 4-C$_5$NF$_4$, 0 kcal/mol (we list the energy of the most stable rotamer). Thus, the observed isomer is the least stable energetically, and therefore must be a kinetic product. These relative energies are very similar to those calculated for NiF(C$_5$F$_4$N)(PMe$_3$)$_2$.[45]

DISCUSSION

Complexes **1** and **1a** are well known to act as sources of the very reactive fragment Tp′Rh(PMe$_3$) by photochemical elimination of H$_2$ and thermal elimination of CH$_4$, respectively.[17,19] To our surprise, the complexes were selective for the activation of B−H, Si−H, and C−F bonds with respect to the C−H bonds within the ligands (Table 3, Scheme 2). Rhodium fluorides, rhodium boryls, and rhodium silyls were therefore the major products in the reactions investigated. Notably, pentafluoropyridine and tetrafluoropyridine undergo C−F activation, but C$_6$F$_6$ does not react in this way, nor does it form an η^2-C$_6$F$_6$ complex, so enabling us to use it as an inert solvent.

Trans Influence and Thermodynamics. Trans influence is related to the σ-donor strength of the ligands.[46] The results illustrate the effect of trans influence on Rh−N distances and coupling constants. The shortest Rh−N distance for N trans to F, 2.0452(17) Å, is followed by N trans to P (2.114 to 2.124 Å), next trans to C$_5$NF$_4$ (2.1869(17) Å), then trans to H (2.241(2) and 2.247(2) Å), and finally trans to boryl or silyl (2.297(2) and 2.299(3) Å). The J_{RhP} coupling constants for Tp′Rh(PMe$_3$)(E)H follow the order E = C$_5$NF$_4$ (127 Hz) < H (138 Hz) < H$_{3-m}$SiR$_m$ (140 Hz) < B(OR$_2$) (145 Hz), consistent with the order of trans influence.

The boryl product **2** is inert with respect to reaction with benzene, even at 130 °C. DFT calculations demonstrate that this reaction is thermodynamically unfavorable (eq 2). The primary C−H bonds in the ligand did not compete with the clean formation of rhodium-boryl hydrides. The methyl groups of HBpin are hindered and it is already known that activation of hindered C−H bonds (e.g., in neopentane) by Tp′Rh does not occur,[11a] and the calculations show that the product formed by methyl C−H activation is unstable with respect to **2**. Similarly, the calculations indicate that the silyl complexes **3** and **4** are thermodynamically stable with respect to reaction with benzene (eq 2).

Kinetics. The kinetic studies show that the rate of formation of product in the photochemical reactions of **1** with monochromatic radiation is independent of the substrate concentration, whereas the rate in the thermal reactions of **1a** is linearly dependent on [substrate]. Thus, the photochemical kinetics are consistent with initial loss of H$_2$ followed by reaction with substrate (eq 1). In contrast, we interpret the kinetics of **1a** under thermal conditions in terms of κ^3−κ^2 isomerization of the Tp′ ligand with concomitant conversion to an η^2-methane complex in a pre-equilibrium followed by rate-determining bimolecular reaction with substrate (Scheme 4), as seen in the reaction of Tp′Rh(CNneopentyl)(CH$_3$)H with benzene.[39] Evidence for a comparable κ^3−κ^2 isomerization has been found in Tp′Rh(PPh$_3$)$_2$.[22]

Selectivity and Competition. *Intramolecular Selectivity.* The examples above provide evidence that intramolecular competition strongly favors B−H or Si−H activation over C−H activation of alkyl groups. Similarly, Si−H activation and C−F activation can occur in the presence of a competing aromatic C−H bond, but the selectivity is much lower. The photochemical reactions of **1** in neat C$_5$F$_5$N proved to be regioselective for C−F activation in the ortho position; two conformers of **6** were observed in the reaction. The DFT calculations show that the ortho selectivity of C−F activation must arise from a kinetic preference. Such selectivity has been reported several times previously.[4,47] The reaction of tetrafluoropyridine generates a mixture of C−H and C−F bond activation products. In contrast, reactions of [Tp′Rh(CNR)] and [Tp′Rh(PMe$_3$)] with partially fluorinated benzenes generate the C−H activation product exclusively and the same applies to [CpRh(PMe$_3$)] and [Cp*Rh(PMe$_3$)], RhH(PEt$_3$)$_3$ and other examples.[13a,18a,48] Nevertheless, C−F bond activation with tetrafluoropyridine has been observed at Rh{Si(OEt)$_3$}(PEt$_3$)$_3$, Rh(SiPh$_3$)(PMe$_3$)$_3$, and [Ni(PEt$_3$)$_2$][4,47a,c,49]

The well-established unimolecular hopping mechanism that provides the basis of selectivity between different C−H groups of

DOI: 10.1021/ja5113172
J. Am. Chem. Soc. 2015, 137, 1258−1272

alkanes[50] offers a model for the intramolecular selectivity as illustrated in Scheme 5 for phenylsilane. The ability of silanes and boranes to form σ-complexes is well known.[1,2,51] We propose that the selectivity originates in a combination of equilibration between σ-complexes and/or π-complexes (k_1 and k_{-1}) and differential rates of oxidative cleavage (k_{SiH}^{oc} and k_{CH}^{oc}). If fast equilibration occurs between Rh(σ-Si−H) and Rh(η^2-$C_6H_5SiH_3$) complexes, the Curtin-Hammett principle applies and the product ratio is determined by the relative rates for oxidative cleavage (k_{SiH}^{oc} vs k_{PhH}^{oc}) and the position of equilibrium. The experiments above together with earlier data establish that the rates of interconversion of oxidative cleavage products (k_2 and k_{-2}) are negligible. The intramolecular selectivities are listed in Table 3.

Scheme 5. Intramolecular Competition for Photochemical Reactions of 1 (oc = Oxidative Cleavage)

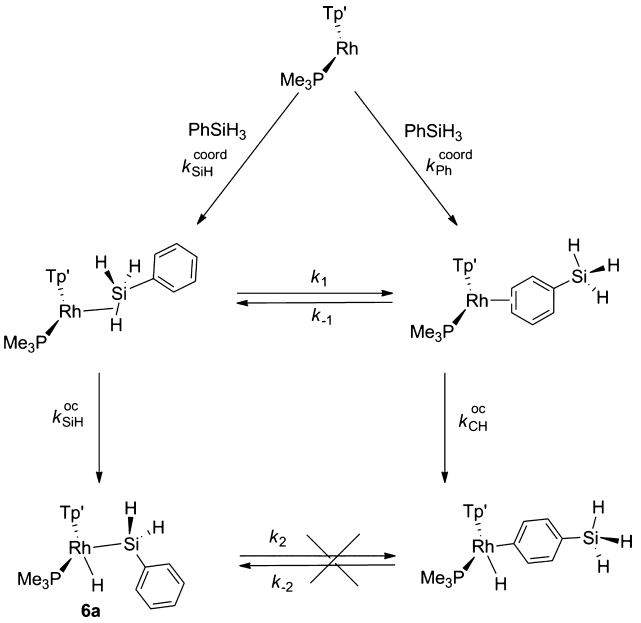

Scheme 6. Intermolecular Competition Mechanism for Photochemical Reactions of 1

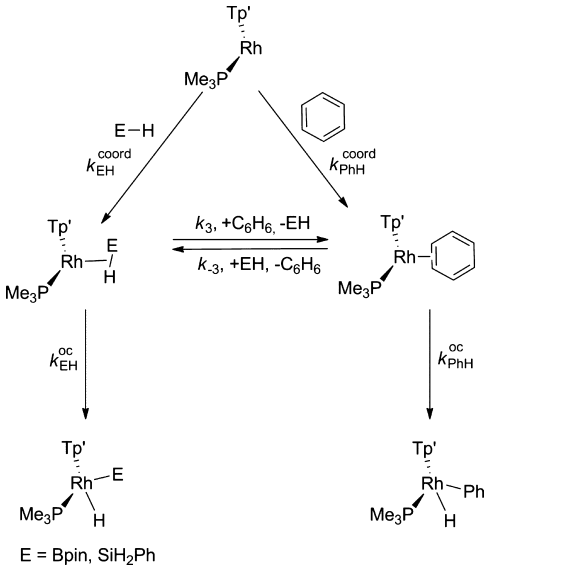

Intermolecular Selectivity. Photochemical intermolecular competition reactions in C_6F_6 solution allowed the determination of a scale for the activation of the "hetero-bonds". The kinetic selectivity follows the sequence shown in Table 8 that can be compared to that already established for reactivity of different types of C−H bond toward [Tp′Rh(PMe_3)]. The kinetic selectivity in the previously reported series of photochemical experiments spans a factor of ca. 25.[19]

The rates of reaction of $PhSiH_3$ and HBpin are comparable to those of CH_2F_2 and pentane, respectively, and that of pentafluoropyridine is similar to cyclopentane. There are few comparable sets of competition experiments; CpRh(PPh_3)(C_2H_4) showed no significant selectivity between H−Bpin, H−C_6F_5, and H−$SiMe_2Et$ substrates.[21] The sequence for Ru(DuPHOS)$_2$ is established as H−SiH_2Ph > H−Bpin > H−C_6F_5 by laser flash photolysis.[52] In Scheme 6, we illustrate the mechanistic basis of intermolecular selectivity for a general substrate E−H in a way related to that for intramolecular competition. The selectivity for E−H vs benzene occurs as a result of competition between three pairs of rate constants: (1) formation of the E−H σ-complex vs Rh(η^2-C_6H_6), (2) interconversion of the these two species by bimolecular substitution (k_3 and k_{-3}), and (3) rates of oxidative cleavage (k_{SiH}^{oc} and k_{CH}^{oc}). Their relative importance depends on whether equilibration occurs between Rh(σ-E−H) and Rh(η^2-C_6H_6) complexes. Under conditions where no equilibration occurs, selection takes place by initial coordination of substrate (relative values k_{EH}^{coord} vs k_{PhH}^{coord}). If fast equilibration occurs, expected only at high concentration of substrate, the Curtin−Hammett principle applies once more, and the product ratio is determined by the relative rates for oxidative cleavage (k_{EH}^{oc} vs k_{PhH}^{oc}) and the position of equilibrium. In the absence of equilibration, the selectivity is given by the ratio of coordination rate constants multiplied by the concentration ratio k_{EH}^{coord} [EH]/k_{PhH}^{coord}[C_6H_6]. Our photochemical competition reactions were performed with 0.5 M concentrations of each substrate, which is probably insufficient for fast equilibration. We can exclude the effect of secondary photolysis on the Rh(III) products because the reactions were only taken to 40% conversion. Thermal interconversion between the Rh(III) products does not occur.

Table 8. Intermolecular Selectivity Derived from Photochemical Competition Reactions

substrate[a]	Si−H ($PhSiH_3$)		C−H (C_6H_6)		B−H (HBpin)		C−F (C_5NF_5)	
k_{rel}	2.3		1		0.36		0.07	
substrate[b]	CH_2F_2	C_6H_6	HCCPh	pentane	CH_4	CH_3CF_3	$(CH_3)_2CO$	c-C_5H_{10}
k_{rel}	1.6	1	0.47	0.41	0.39	0.20	0.16	0.063

[a]This work. [b]From ref 19.

DOI: 10.1021/ja5113172
J. Am. Chem. Soc. 2015, 137, 1258−1272

CONCLUSIONS

These experiments show that the [Tp′Rh(PMe$_3$)] system can activate a much wider variety of bonds than had been previously realized, opening up the possibilities of new applications through C−F, B−H, and Si−H bond activation via photolysis of Tp′Rh(PMe$_3$)H$_2$ or thermal reaction with Tp′Rh(PMe$_3$)(CH$_3$)-H. Although [Tp′Rh(PMe$_3$)] is capable of activating alkanes, it proves highly selective in reactions involving intramolecular competition between E−H and C−H bond activation. The compounds with Rh−B and Rh−Si bonds do not react with benzene to form Tp′Rh(PMe$_3$)(Ph)H because the reaction is thermodynamically unfavorable according to DFT calculations. The Rh−Ph and Rh−Si BDEs are calculated to be similar but considerably smaller than the Rh−B BDE. We observe C−F activation of pentafluoropyridine with ortho selectivity, but hexafluorobenzene is unreactive and can be used as an inert solvent. The wide scope and selectivity of the reactivity of **1** and **1a** should be recognized when considering their applications and those of related C−H activators.

Mechanism. The investigations of the photochemical mechanism for **1** indicate reductive elimination of H$_2$ prior to substrate attack in a dissociative mechanism. We can also make an informed judgment that this reaction takes place from the ground state of Tp′Rh(PMe$_3$) rather from an excited state of **1**. The excited state of **1** would need to have a lifetime of ≥500 ps to react with substrates under our reaction conditions (1 M substrate in C$_6$F$_6$) whereas it is known that ruthenium phosphine dihydride complexes undergo prompt photodissociation within 10 ps of laser excitation.[53] It is also established that photodissociation of CO from Tp′Rh(CO)$_2$ occurs within 100 fs.[6d] The reaction kinetics of **1a** demonstrate a bimolecular mechanism resulting in second-order kinetics. We postulate initial decoordination of one pyrazolyl arm of **1a** and concomitant conversion to a methane complex. The substrate attacks this intermediate with loss of methane and recoordination of the pyrazolyl ensues (Scheme 4).

Intramolecular Selectivity. With HBpin as substrate, complete intramolecular selectivity for the activation of the B−H bond is observed, leaving the methyl groups untouched. With Et$_2$SiH$_2$, there is complete selectivity for the Si−H bond under thermal conditions and almost complete selectivity under photochemical conditions. The selectivity for the Si−H bond over the C−H bonds of PhSiH$_3$ is ca. 3−4 under both photochemical and thermal conditions. The DFT calculations show that there is a thermodynamic preference for intramolecular B−H over C−H activation and for Si−H over C−H activation. Taken together with results obtained earlier,[13c] it is now evident that [Tp′Rh(PMe$_3$)] shows strong selectivity in intramolecular competition for C−H over C−X (X = OR, F, CN) bond activation where the substrate contains one C−X bond, but it reacts with B−H or Si−H bonds in preference to C−H bonds. It has been observed previously that the preference for C−H activation can be overridden in the presence of more than one X group, as in CH$_2$Cl$_2$.[54] Tetrafluoropyridine offers four C−F bonds, and the reaction results in a mixture of 20% C−F and 80% C−H oxidative addition. We postulate that the intramolecular selectivity arises from initial competition of the [Tp′Rh(PMe$_3$)] for the substrate *and* hopping between different σ and π coordination in intermediate Rh(I) species (Scheme 5).

Intermolecular Selectivity. The kinetic selectivity of [Tp′Rh(PMe$_3$)] has been determined through photochemical competition experiments on **1** with benzene as standard and follows the order Si−H (PhSiH$_3$) > C−H(C$_6$H$_6$) > B−H (HBpin) ≫ C−F (C$_5$NF$_5$), these reactions and those previously published shown in Table 8 span a factor of 37 in rates. Intermolecular selection occurs at the stage of initial reaction of [Tp′Rh(PMe$_3$)] with substrate when the substrate is dilute, but the selection may be different at high concentration when equilibration between Rh^I(σ-E−H) and Rh^I(η^2-C$_6$H$_6$) complexes may occur (Scheme 6). The intermolecular selectivity for PhSiH$_3$ over benzene has also been studied in thermal reactions of **1a**. In dilute solutions in THF, there is exclusive preference for Si−H activation, but in a 50:50 mixture (by volume), Si−H activation is preferred by a factor of 5.1:1.

EXPERIMENTAL SECTION

General Procedures. All operations were performed on a high-vacuum line (10^{-5} mbar), under an argon atmosphere on a standard Schlenk (10^{-3} mbar) line, or in a glovebox. Solvents for general use were of AR grade, dried by distillation over sodium and stored under Ar in ampules fitted with a Young's PTFE stopcock. Hexane was collected from the solvent purification system and dried again by distillation. Deuterated solvents were dried by stirring over potassium and distilled under high vacuum into small ampules with potassium mirror. Complex **1** and **1a** were synthesized following the literature procedures.[17,19] The fluoropyridines, hexafluorobenzene (99.5%), and silanes used were purchased from Aldrich and dried over molecular sieves. HBpin (also Aldrich) was purified by vacuum distillation. Photochemical reactions at room temperature were performed in pyrex NMR tubes fitted with Young's PTFE stopcocks by using a Philips 125 W medium-pressure mercury vapor lamp with a water filter (5 cm). CHN analysis was performed by the CENTC Elemental Analysis facility at the University of Rochester.

NMR spectra were recorded in tubes fitted with Young's PTFE stopcocks on a Bruker AMX500 spectrometer in York or on Bruker Avance 400 or Avance 500 spectrometers in Rochester. All ^{1}H and ^{13}C chemical shifts are reported in ppm (δ) relative to tetramethylsilane and referenced using the chemical shifts of residual protio solvent resonances (benzene, δ 7.16 for ^{1}H and δ 128.06 for ^{13}C). The ^{31}P{^{1}H} NMR spectra were referenced to external H$_3$PO$_4$. ^{11}B NMR spectra to external BF$_3$·Et$_2$O, ^{19}F spectra to external CFCl$_3$ and ^{29}Si spectra to external TMS. 2D NMR spectra were recorded with a standard HMQC pulse program varying the values of J_{XH} from 2 to 200 Hz.

We described our setup for laser photolysis within an NMR spectrometer in recent papers.[55] Laser photolysis was carried out with a pulsed Nd:YAG laser (Continuum Surelite II) fitted with a frequency tripling crystal. Operating conditions were typically 10 Hz repetition rate, flash lamp voltage 1.49 kV, Q-switch delay increased from the standard to 320 μs yielding a laser power of 85 mW when operating at 355 nm. A very dilute sample of Ru(CO)$_2$(dppe)$_2$H$_2$ or Ru(CO)$_2$(dppe)(PPh$_3$) (dppe = Ph$_2$PCH$_2$CH$_2$PPh$_2$) in C$_6$D$_6$ was used for laser alignment, with para-hydrogen amplification in real time. NMR spectra were recorded on a Bruker Avance wide-bore 600 MHz spectrometer.

The LIFDI mass spectra were measured on a Waters Micromass GCT Premier orthogonal time-of-flight instrument set to one scan per second with resolution power of 6000 fwhm and equipped with a LIFDI probe from LINDEN GmbH. The design is very similar to that described by Gross et al.[56] LIFDI m/z values are accurate to 0.01 Da. EI mass spectra were measured on the same instrument under high resolution conditions. Mass to charge ratios are quoted for ^{11}B, ^{28}Si.

Diffraction data were collected at 110 K on an Agilent SuperNova diffractometer with Mo Kα radiation (λ = 0.71073 Å). Data collection, unit cell determination and frame integration were carried out with "CrysalisPro". Absorption corrections were applied using crystal face-indexing and the ABSPACK absorption correction software within CrysalisPro. Structures were solved and refined using Olex2[57] implementing SHELX algorithms. Structures were solved by either Patterson or direct methods using SHELXS-97 and refined by full-

DOI: 10.1021/ja5113172
J. Am. Chem. Soc. 2015, 137, 1258−1272

Table 9. Refinement Data for Complexes 2, 3, and 7·C_5NF_5

	Tp′Rh(PMe_3)(Bpin)H (**2**)	Tp′Rh(PMe_3)($SiEt_2H$)H (**3**)	Tp′Rh (PMe_3)(2-C_5NF_4)(FHF)·C_5NF_5 (**7**·C_5NF_5)
formula	$C_{24}H_{44}B_2N_6O_2PRh$	$C_{22}H_{43}BN_6SiPRh$	$C_{28}H_{32}BF_{11}N_8PRh$
M	604.15	564.4	834.31
a/Å	25.996(12)	10.840(7)	34.358(13)
b/Å	10.660(2)	11.533(9)	8.538(3)
c/Å	21.452(5)	13.546(11)	22.805(9)
α/deg	90.00	65.602(8)	90.00
β/deg	101.455(3)	72.784(7)	99.322(4)
γ/deg	90.00	65.226(7)	90.00
V/ Å^3	5819.4(12)	1384.81(18)	6601.3(4)
T/K	110(2)	110(2)	110(2)
space group	$C2/c$	P-1	$C2/c$
Z	8	2	8
μ Mo Kα/mm^{-1}	0.674	0.739	0.663
reflns meas	11082	12496	16457
reflns indep	5832	5656	9556
R_{int}	0.0249	0.0294	0.0252
final R [$I > 2\sigma(I)$]	R_1 = 0.0307	R_1 = 0.0329	R_1 = 0.0356
	wR_2 = 0.0660	wR_2 = 0.0708	wR_2 = 0.0785
final R (all data)	R_1 = 0.0384	R_1 = 0.0414	R_1 = 0.0458
	wR_2 = 0.0699	wR_2 = 0.0764	wR_2 = 0.0831
CCDC no.	1032686	1032687	1032685

matrix least-squares using SHELXL-97. All non-hydrogen atoms were refined anisotropically. Carbon-bound hydrogen atoms were placed at calculated positions and refined using a "riding model". Hydrogen atoms bound to rhodium and silicon were found by difference map and refined. Crystallographic data are listed in Table 9.

Syntheses and NMR Experiments. *Photochemical Reactions of complex **1**.* All of the products were synthesized by irradiating **1** (ca. 10 mg) dissolved in neat substrates (~0.5 mL) except for the reaction of **1** (ca. 10 mg) with $PhSiMe_3$ (6 fold excess) which was performed in C_6F_6 as the solvent. NMR yields were determined as ratios of product:precursor without internal standards. Rh-fluoride and Rh-boryl complexes were partially purified by passing the reaction mixture through a neutral alumina column. This method was ineffective for the Rh-silyl products where other products were formed during photolysis. Crystals were grown by slow evaporation of hexane solutions.

*Thermal Reactions of Complex **1a**.* Solutions of **1a** prepared in THF from Tp′Rh(PMe_3)(Me)Cl and Cp_2ZrH_2 contain some Tp′Rh(PMe_3)-(trihydrofuranyl)H (**1b**, 6–35%), depending on how long the solution was prepared prior to reaction with added substrate. Some Tp′Rh-(PMe_3)(H)Cl is also formed (9–17%), but remains unreactive (see tables in Supporting Information for distributions). HBpin (0.06 mL, 0.413 mmol) was added to the solution of **1a** (20 mg, 0.038 mmol) in THF (0.54 mL) yielding a concentration of HBpin of 0.69 M. The colorless reaction mixture was transferred to a Young's tube and monitored by ^{1}H and ^{31}P{^{1}H} NMR spectroscopy. The reaction was complete in 2 weeks at room temperature to give pale yellow solids after evaporation of the solvent. In the same way, Et_2SiH_2 (0.1 mL, 0.772 mmol) was added to the solution of **1a** in THF (0.5 mL) (concentration of Et_2SiH_2, 1.29 M). Similarly, $PhSiH_3$ (0.1 mL, 0.810 mmol) was added to a solution of **1a** in 0.5 mL THF (concentration of $PhSiH_3$, 1.35 M). The reaction was complete after 9 days at room temperature, resulting in pale yellow precipitate. A white powder was obtained following recrystallization in hexane. The reaction with $PhSiH_3$ under the same conditions proved to be much faster (1 day). Yield by NMR: 86% **4**, 14% Tp′Rh(PMe_3)(H)Cl. The reaction of **1a** (0.019 mmol) with $PhSiMe_3$ (0.6 mL, 3.5 mmol) produced **5** after 20 h at room temperature. The reaction of **1a** with pentafluoropyridine was complete after 2 days at room temperature.

*Tp′Rh(PMe₃)(Bpin)H (**2**).* ^{1}H NMR (C_6D_6, 300 K): δ −16.77 (dd, J_{RhH} = 25.5 Hz, J_{PH} = 30.9 Hz, RhH, fwhm 2.5 Hz),1.16 (s, 6H, BOC−CH_3), 1.21 (s, 6H, BOC−CH_3), 1.35 (d, 9H, J_{PH} = 9 Hz, P(CH_3)$_3$), 2.07 (s, 3H, pzCH_3), 2.29 (s, 3H, pzCH_3), 2.30 (s, 3H, pzCH_3), 2.31 (s, 3H, pzCH_3), 2.41 (s, 3H, pzCH_3), 2.49 (s, 3H, pzCH_3), 4.75 (b, J_{BH} = 121 Hz, 1H, pzBH), 5.54 (s, 1H, pzH), 5.70 (s, 1H, pzH), 5.86 (s, 1H, pzH). ^{13}C NMR (C_6D_6): δ 12.73, 13.07, 13.23, 16.38, 17.42, 17.53 (s, pzCH_3), 21.50 (d, J_{PC} = 32 Hz, P(CH_3)$_3$), 22.0, 25.2, 26.3, 27.7 (s, BOC−CH_3), 81.16 (s, BOC), 105.4 (d, J_{PC} = 3 Hz, pzCH),105.8 (s, pzCH), 106.1 (s, pzCH), 143.2 (s, pzCq), 143.5 (s, pzCq), 144.2 (s, pzCq), 146.6 (s, pzCq), 149.6 (d, pzCq), 150.0 (s, pzCq). ^{11}B NMR (C_6D_6): δ 39.25 (b, Rh−B), −8.72 (b, pzB−H). ^{31}P{^{1}H} NMR (C_6D_6): δ 5.25, (d, J_{RhP} = 145 Hz). LIFDI-MS: m/z 604.22 (100%, M$^+$). EI-MS m/z 604.2609 (M$^+$−H) 5%, (calcd for $C_{24}H_{44}N_6{}^{11}B_2O_2PRh$ 604.2513, difference −9.6 mDa). Anal. Calcd for $C_{24}H_{44}B_2N_6O_2PRh$: C, 47.71; H, 7.34; N, 13.91. Calcd for $C_{24}H_{44}B_2N_6O_2PRh$·0.1 hexane: C, 48.22; H, 7.47; N, 13.71. Found: C, 48.38; H, 7.40; N, 13.61. Hexane is observed in the ^{1}H NMR spectrum.

*Tp′Rh(PMe₃)(SiEt₂H)H (**3**).* ^{1}H NMR (C_6D_6, 300 K): δ −17.89 (dd, J_{PH} = 32.3 Hz, J_{RhH} = 20.3 Hz, RhH), 0.87 (m, 6H, $SiCH_3$), 1.25 (d, 9H, J_{PH} = 11 Hz, P(CH_3)$_3$), 1.43 (m, 4H, $SiCH_2$), 2.13 (s, 3H, pzCH_3), 2.19 (s, 3H, pzCH_3), 2.22 (s, 3H, pzCH_3), 2.30 (s, 3H, pzCH_3), 2.39 (s, 3H, pzCH_3), 2.52 (s, 3H, pzCH_3), 4.36 (bd, J_{PH} = 15 Hz, Si−H), 5.56 (s, 1H, pzH), 5.64 (s, 1H, pzH), 5.82 (s, 1H, pzH). ^{29}Si NMR (C_6D_6): δ 31.84 (b, Rh−Si). ^{31}P{^{1}H} NMR (C_6D_6): δ 0.87, (d, J_{RhP} = 140 Hz). LIFDI-MS: m/z 564.19 (100%, M$^+$). Anal. Calcd for $C_{22}H_{43}BN_6PRhSi$: C, 46.82; H, 7.68; N, 14.89. Calcd for $C_{22}H_{43}BN_6PRhSi$·0.1 hexane: C, 47.37; H, 7.81; N, 14.67. Found: C, 47.23; H, 7.69; N, 14.57.

*Tp′Rh(PMe₃)(SiPhH₂)H (**4**).* ^{1}H NMR (C_6D_6, 300 K): δ −16.7 (dd, J_{PH} = 30.6 Hz, J_{RhH} = 20 Hz, RhH), 1.17 (d, 9H, J_{PH} = 9 Hz, P(CH_3)$_3$), 2.08 (s, 3H, pzCH_3), 2.22 (s, 3H, pzCH_3), 2.27 (s, 3H, pzCH_3), 2.31 (s,3H, pzCH_3), 2.32 (s, 3H, pzCH_3), 2.34 (s, 3H, pzCH_3), 4.95 (bdd, Si−H), 5.27 (m, Si−H), 5.39 (s, 1H, pzH), 5.69 (s, 1H, pzH), 5.79 (s, 1H, pzH), 7.12 (m, 3H, Ph), 7.87 (d, 2H, Ph). ^{29}Si NMR (C_6D_6): δ −15.8 (b, Rh−Si). ^{31}P{^{1}H} NMR (C_6D_6): δ 1.9 (d, J_{RhP} = 131 Hz). LIFDI-MS: m/z 584.15 (100%, M$^+$). Anal. Calcd for $C_{24}H_{39}BN_6PRhSi$: C, 49.33; H, 6.73; N, 14.38. Calcd for $C_{24}H_{39}BN_6PRhSi$·0.1 hexane: C, 49.83; H, 6.87; N, 14.17. Found: C, 50.01; H, 6.79; N, 13.88.

*Tp′Rh(PMe₃)(C₆H₄SiMe₃)H (**5**, o, m, and p Forms).* ^{1}H NMR (C_6H_6, 300 K): δ −16.86, −16.87, −16.91 (dd, J_{PH} = 30.2 Hz, J_{RhH} = 25, 24.7, 25.2 Hz, *o,m,p* RhH), 0.13, 0.29, 0.40 (s, *o,m,p* Si(CH_3)$_3$), 1.14 (d, 9H, J_{PH} = 10 Hz, *o,m,p* P(CH_3)$_3$), 1.68, 1.72 (two overlapping), 1.73, 2.03, 2.04, 2.05, 2.12 (two overlapping), 2.16, 2.20, 2.21, 2.22, 2.26 (two overlapping), 2.26 (two overlapping), 2.35, 2.37 (two overlapping) (s, 3H, *o,m,p* pzCH_3), 5.45, 5.46, 5.49, 5.67, 5.68 (two overlapping), 5.86, 5.88, 5.91, (s, 1H, *o,m,p* pzH), 6.87–7.93 (m, *o,m,p* phenyl H). ^{29}Si NMR

DOI: 10.1021/ja5113172
J. Am. Chem. Soc. 2015, 137, 1258–1272

(C_6D_6): δ − 6.12 (br). $^{31}P\{^1H\}$ NMR (C_6D_6): δ 2.7, 2.8, 3.1 (d, J_{RhP} = 145.7, 146.5, 146.3 Hz). See also Table 2.

*Tp′Rh(PMe$_3$)(2-C$_5$NF$_4$)F, Major Rotamer of **6**.* ^1H NMR (C_6D_6, 300 K): δ 1.11 (d, J_{PH} = 10.1 Hz, 9H, P(CH_3)$_3$), 1.37 (s, 3H, pzCH_3), 1.93 (s, 3H, pzCH_3), 2.07 (s, 3H, pzCH_3), 2.18 (s, 3H, pzCH_3), 2.24 (s, 3H, pzCH_3), 2.47 (s, 3H, pzCH_3), 5.44 (s, 1H, pzH), 5.53 (s, 1H, pzH), 5.63 (s, 1H, pzH). $^{19}F\{^1H\}$ NMR (C_6D_6): δ −85.9 (m, 1F), −133.0 (m, 1F), −148.3 (m, 1F), −169.0 (m, 1F), −428.8 (br d, 1F, J_{RhF} = 185 Hz, Rh*F*). $^{31}P\{^1H\}$ NMR (C_6D_6): δ 6.67, (dd, J_{RhP} = 128.7 Hz, J_{PF} = 17 Hz). ^{13}C NMR (C_6D_6): δ 12.5, 12.6, 12.7, 12.8, 15.0, 16.6 (s, pzCH_3), 14.7 (dd, J_{PC} = 33 Hz, P(CH_3)$_3$), 107.0 (d, J_{PC} = 4.5 Hz, pzCH), 108.1 (s, pzCH), 108.2 (s, pzCH), 142.8 (d, J_{PC} = 3.3 Hz, pzCq), 144.1 (s, pzCq), 146 (s, pzCq), 151.2 (d, J_{PC} = 4.2 Hz, pzCq), 152 (s, pzCq), 152.7 (s, pzCq). Signals assignable to the five carbons of C_5F_4N group were not detected because of multiple coupling with fluorines.

*Tp′RhF(PMe$_3$)(2-C$_5$NF$_4$)F, Minor Rotamer of **6**.* ^1H NMR (C_6D_6, 300 K): δ 1.04 (d, J_{PH} = 9.6 Hz, 9H, P(CH_3)$_3$), 1.32 (s, 3H, pzCH_3), 1.78 (s, 3H, pzCH_3), 1.98 (s, 3H, pzCH_3), 2.13 (s, 3H, pzCH_3), 2.22 (s, 3H, pzCH_3), 2.49 (s, 3H, pzCH_3), 5.42 (s, 1H, pzH), 5.54 (s, 1H, pzH), 5.62 (s, 1H, pzH). $^{19}F\{^1H\}$ NMR (C_6D_6): δ −84.6 (m, 1F), −129.8 (m, 1F), −146.6 (m, 1F), −168.5 (m, 1F). $^{31}P\{^1H\}$ NMR (C_6D_6): δ 2.4, (dt, J_{RhP} = 126 Hz, J_{PF} = 18 Hz). ^{19}F NMR (toluene-d_8, 235 K): additional resonance δ −455.4 (br d, 1F, J_{RhF} = 183 Hz, Rh*F*). LIFDI-MS: *m*/*z* 645.12 (100%, M^+), 625.10 (20%, [M^+]−HF). EI-MS: *m*/*z* 645.1466 (M^+) 2.5% (calculated for $C_{23}H_{31}{}^{11}BN_7F_5PRh$ 645.1451, difference −1.5 mDa).

*Tp′Rh(PMe$_3$)(2-C$_5$NF$_4$)(FHF) (**7**).* ^1H NMR (toluene-d_8, 300 K): δ 1.13 (d, 9H, P(CH_3)$_3$), 1.39 (s, 3H, pzCH_3), 1.83 (s, 3H, pzCH_3), 2.11 (s, 3H, pzCH_3), 2.21 (s, 3H, pzCH_3), 2.25 (s, 3H, pzCH_3), 2.42 (s, 3H, pzCH_3), 5.40 (s, 1H, pzH), 5.49 (s, 1H, pzH), 5.59 (s, 1H, pzH), 11 (b, 1H, FHF). ^{13}C NMR (toluene-d_8): δ 12.4, 12.43, 13.5, 14.5, 14.8, 16.5 (s, pzCH_3), 16.08 (dd, J_{PC} = 32.5 Hz, J_{RhC} = 3 Hz, P(CH_3)$_3$), 107.0 (d, J_{PC} = 4.4 Hz, pzCH), 108.3 (s, pzCH), 108.4 (s, pzCH), 142.9 (d, J_{PC} = 3 Hz, pzCq), 144 (s, pzCq), 146 (s, pzCq), 151.1 (d, J_{PC} = 4 Hz, pzCq), 151.9 (s, pzCq), 152.8 (s, pzCq). Signals assignable to the five carbons of the C_5F_4N group were not detected. $^{19}F\{^1H\}$ NMR (toluene-d_8, 205 K): δ −84.9 (m, 1F), −133.5 (m, 1F), −147.1 (m, 1F), −167.1 (m, 1F), −178.7 (d, J_{RhF} = 447.6 Hz, FH*F*), −398.9 (b, 1F, Rh*F*). $^{31}P\{^1H\}$ NMR (toluene-d_8, 205 K): δ 6.67, (dd, J_{RhP} = 129 Hz, J_{PF} = 17 Hz). LIFDI-MS: *m*/*z* 645.12 (100%, M^+−HF).

*Tp′Rh(PMe$_3$)(C$_5$NF$_4$)H (**8**).* ^1H NMR (C_6D_6, 300 K): δ −15.51 (ddd, J_{PH} = 25 Hz, J_{FH} = 19 Hz, J_{RhH} = 14 Hz, 1H, RhH), 0.94 (d, 9H, J_{PH} = 10 Hz, P(CH_3)$_3$), 1.48 (s, 3H, pzCH_3), 1.77 (s, 3H, pzCH_3), 2.01 (s, 3H, pzCH_3), 2.14 (s, 3H, pzCH_3), 2.16 (s, 3H, pzCH_3), 2.33 (s, 3H, pzCH_3), 4.68 (b, J_{BH} = 113 Hz, 1H, pzBH), 5.34 (s, 1H, pzH), 5.55 (s, 1H, pzH), 5.80 (s, 1H, pzH). $^{19}F\{^1H\}$ NMR (C_6D_6): δ −100.6 (m, 2F), −125.2 (m, 2F). $^{31}P\{^1H\}$ NMR (C_6D_6): δ −2.33, (dd, J_{RhP} = 127 Hz, J_{PF} = 20 Hz).

*Tp′Rh(PMe$_3$)(C$_5$NF$_3$H)F (**8a**).* ^1H NMR (C_6D_6, 300 K): δ 1.16 (d, 9H, J_{PH} = 11.1 Hz, P(CH_3)$_3$), 1.42 (s, 3H, pzCH_3), 1.84 (s, 3H, pzCH_3), 2.10 (s, 3H, pzCH_3), 2.24 (s, 3H, pzCH_3), 2.26 (s, 3H, pzCH_3), 2.46 (s, 3H, pzCH_3), 5.48 (s, 1H, pzH), 5.56 (s, 1H, pzH), 5.64 (s, 1H, pzH), 6.20 (m, 1H, pyrH). $^{19}F\{^1H\}$ NMR (C_6D_6): δ −111.6 (m, 1F), −126.9 (m, 1F), −146.3 (m, 1F), −430.1 (d, J_{FRh} = 181.3 Hz, 1F, RhF). $^{31}P\{^1H\}$ NMR (C_6D_6): δ 4.6, (dd, J_{RhP} = 132 Hz, J_{PF} = 17 Hz). In addition, a minor rotamer is detected (ca. 5% of **8a**). ^{31}P NMR (C_6D_6): δ 2.2 (J_{PH} = 134 Hz). ^{19}F NMR (C_6D_6): δ −458.6 (J_{PH} = 187 Hz). LIFDI-MS: *m*/*z* 626.17 (100%, M^+−H), 608.18 (35%, M^+−F).

Effect of Concentration on Photochemistry. A stock solution was made up of **1** (8 mM) in C_6F_6. An aliquot of stock was transferred to each of four NMR tubes, followed by a measured quantity of HBpin and the solutions were each made up to the same overall volume, giving concentrations of HBpin of 0.37, 0.75, 1.25, and 1.87 M. A similar procedure was used for the $PhSiH_3$ reactions giving concentrations of 0.44, 0.88, 1.47, and 2.20 M. The solutions were irradiated with broad-band radiation with a λ > 300 nm cutoff filter and NMR spectra ($^1H\{^{31}P\}$ and $^{31}P\{^1H\}$ with inverse gated decoupling) were recorded every 20 min for 1 h.

Photochemical Kinetics with Monochromatic Photolysis. In order to monitor the photochemical conversion as a function of time, a stock solution was made up of **1** (6 mM) in C_6F_6. An aliquot was transferred to an NMR tube and HBpin added to give a concentration of 0.4 M. The same stock was used to make up a solution with $PhSiH_3$ (0.45 M). The solutions were irradiated *in situ* with the laser at 355 nm and NMR spectra ($^1H\{^{31}P\}$ and $^{31}P\{^1H\}$ with inverse gated decoupling) were monitored at intervals up to 50% conversion. For intermolecular competition reactions, a stock solution was made up of **1** (6 mM) in C_6F_6 with 0.5 M of C_6H_6 and 0.5 M of competing substrate (HBpin or $PhSiH_3$). For competition between benzene and pentafluoropyridine, the concentrations of benzene and pentafluoropyridine were 0.5 M and 1.5 M, respectively. The solution was irradiated *in situ* and NMR spectra were monitored as above.

*Kinetics and Experimental Simulations of Reaction of **1a** with PhSiH$_3$.* Reaction rates were monitored by $^{31}P\{^1H\}$ NMR spectroscopy with inverse gated decoupling at 21 °C in six experiments with different concentrations of phenyl silane ([$PhSiH_3$] = 0−8.11 M). For each experiment, **1a** was prepared as described previously from Tp′Rh(PMe$_3$)MeCl (10 mg) and Cp_2ZrH_2.[18] This procedure also results in the formation of some Tp′Rh(PMe$_3$)(H)Cl, but this product does not change during the subsequent reaction. The preparation of **1a** also produced some Tp′Rh(PMe$_3$)(trihydrofuranyl)H (**1b**) due to reaction with THF. Both of these react with $PhSiH_3$ to give H−SiH_2Ph and H−$C_6H_4SiH_3$ activation products. Each sample contained a total volume of 0.6 mL, with 0.0, 0.1, 0.2, 0.3, 0.4, and 0.6 mL of $PhSiH_3$ being mixed with THF.

Simulations were carried out for the reactions of **1a** with $PhSiH_3$ in THF solution using KINSIM/FITSIM software.[58] The rate constant k_2 was obtained from the first-order reaction of **1a** in neat THF after dividing the observed first-order rate constant by the concentration of neat THF (12.33 M) and used in the subsequent simulations in the reactions with $PhSiH_3$. The subsequent data treatment is described in the Results section.

Computational Methods. X-ray crystallographic structures were used as the starting points for the calculations. The Tp′ ligand was modeled with all substituents.[13b] The gas-phase structures were fully optimized in redundant internal coordinates,[59] with density functional theory (DFT) and the B3LYP functional.[60] All calculations were performed using the Gaussian03 package.[61] The Rh and P atoms were represented with the effective core pseudopotentials of the Stuttgart group and the associated basis sets improved with a set of f-polarization functions for Rh (R = 1.350)[62] and a set of d-polarization functions for P (R = 0.387).[63] The remaining atoms (C, H, N, and B) were represented by a 6-31G(d,p) basis set.[64] The geometry optimizations were performed without symmetry constraints. The optimizations for bond energies (all the radicals and molecules) were performed with the M06-2X functional, a 6-31g** basis set, and the effective core potential for Rh and P as above.[13c,65]

■ ASSOCIATED CONTENT

Supporting Information

NMR spectra, effect of concentration on formation of **2** and **4**, rates of photochemical reaction in competition reactions, coordinates for DFT calculations, complete ref 61, kinetic data and fitting parameters for reactions of **1a**, and CIF files for crystal structures. This material is available free of charge via the Internet at http://pubs.acs.org.

■ AUTHOR INFORMATION

Corresponding Authors

*jones@chem.rochester.edu

*robin.perutz@york.ac.uk

Notes

The authors declare no competing financial interest.

■ ACKNOWLEDGMENTS

We are grateful to EPSRC for funding and Dr. Naser Jasim and Dr. Estela Haldon Hermoso for experimental assistance.

DOI: 10.1021/ja5113172
J. Am. Chem. Soc. 2015, 137, 1258−1272

Acknowledgment is made to the U.S. Department of Energy for support, grant FG02-86ER13569.

REFERENCES

(1) (a) Corey, J. Y.; Braddock-Wilking, J. *Chem. Rev.* **1999**, *99*, 175. (b) Corey, J. Y. *Chem. Rev.* **2011**, *111*, 863.

(2) Mkhalid, I. A. I.; Barnard, J. H.; Marder, T. B.; Murphy, J. M.; Hartwig, J. F. *Chem. Rev.* **2010**, *110*, 890.

(3) Johansson, L.; Tilset, M.; Labinger, J. A.; Bercaw, J. E. *J. Am. Chem. Soc.* **2000**, *122*, 10846.

(4) Clot, E.; Eisenstein, O.; Jasim, N.; Macgregor, S. A.; McGrady, J. E.; Perutz, R. N. *Acc. Chem. Res.* **2011**, *44*, 333.

(5) (a) Trofimenko, S. *Acc. Chem. Res.* **1971**, *4*, 17. (b) Trofimenko, S. *Chem. Rev.* **1993**, *93*, 943. (c) Crossley, I. R. *Adv. Organomet. Chem.* **2008**, *56*, 199−321.

(6) (a) Purwoko, A. A.; Lees, A. J. *Inorg. Chem.* **1996**, *35*, 675. (b) Purwoko, A. A.; Drolet, D. P.; Lees, A. J. *J. Organomet. Chem.* **1995**, *504*, 107. (c) Lees, A. J. *J. Organomet. Chem.* **1998**, *554*, 1. (d) Blake, A. J.; George, M. W.; Hall, M. B.; McMaster, J.; Portius, P.; Sun, X. Z.; Towrie, M.; Webster, C. E.; Wilson, C.; Zaric, S. D. *Organometallics* **2008**, *27*, 189. (e) Asplund, M. C.; Snee, P. T.; Yeston, J. S.; Wilkens, M. J.; Payne, C. K.; Yang, H.; Kotz, K. T.; Frei, H.; Bergman, R. G.; Harris, C. B. *J. Am. Chem. Soc.* **2002**, *124*, 10605. (f) Bromberg, S. E.; Yang, H.; Asplund, M. C.; Lian, T.; McNamara, B. K.; Kotz, K. T.; Yeston, J. S.; Wilkens, M.; Frei, H.; Bergman, R. G.; Harris, C. B. *Science* **1997**, *278*, 260.

(7) (a) Cristobal, C.; Hernandez, Y. A.; Lopez-Serrano, J.; Paneque, M.; Petronilho, A.; Poveda, M. L.; Salazar, V.; Vattier, F.; Alvarez, E.; Maya, C.; Carmona, E. *Chem.—Eur. J.* **2013**, *19*, 4003. (b) Valpuesta, J. E. V.; Alvarez, E.; Lopez-Serrano, J.; Maya, C.; Carmona, E. *Chem.—Eur. J.* **2012**, *18*, 13149. (c) Conejero, S.; Esqueda, A. C.; Valpuesta, J. E. V.; Alvarez, E.; Maya, C.; Carmona, E. *Inorg. Chim. Acta* **2011**, *369*, 165. (d) Alvarez, E.; Paneque, M.; Petronilho, A. G.; Poveda, M. L.; Santos, L. L.; Carmona, E.; Mereiter, K. *Organometallics* **2007**, *26*, 1231. (e) Carmona, E.; Paneque, M.; Santos, L. L.; Salazar, V. *Coord. Chem. Rev.* **2005**, *249*, 1729. (f) Paneque, M.; Poveda, M. L.; Carmona, E.; Salazar, V. *Dalton Trans.* **2005**, 1422. (g) Slugovc, C.; Padilla-Martinez, I.; Sirol, S.; Carmona, E. *Coord. Chem. Rev.* **2001**, *213*, 129.

(8) Hessell, E. T.; Jones, W. D. *Organometallics* **1992**, *11*, 1496.

(9) Jones, W. D.; Hessell, E. T. *J. Am. Chem. Soc.* **1993**, *115*, 554.

(10) Wick, D. D.; Jones, W. D. *Organometallics* **1999**, *18*, 495.

(11) (a) Vetter, A. J.; Flaschenriem, C.; Jones, W. D. *J. Am. Chem. Soc.* **2005**, *127*, 12315. (b) Clot, E.; Eisenstein, O.; Jones, W. D. *Proc. Natl. Acad. Sci. U.S.A.* **2007**, *104*, 6939.

(12) Vetter, A. J.; Jones, W. D. *Polyhedron* **2004**, *23*, 413.

(13) (a) Evans, M. E.; Burke, C. L.; Yaibuathes, S.; Clot, E.; Eisenstein, O.; Jones, W. D. *J. Am. Chem. Soc.* **2009**, *131*, 13464. (b) Evans, M. E.; Jones, W. D. *Organometallics* **2011**, *30*, 3371. (c) Jiao, Y. Z.; Evans, M. E.; Morris, J.; Brennessel, W. W.; Jones, W. D. *J. Am. Chem. Soc.* **2013**, *135*, 6994.

(14) (a) Nishiyama, H.; Horihata, M.; Hirai, T.; Wakamatsu, S.; Itoh, K. *Organometallics* **1991**, *10*, 2706. (b) Labinger, J. A.; Osborn, J. A.; Coville, N. J. *Inorg. Chem.* **1980**, *19*, 3236. (c) Lau, K. S. Y.; Fries, R. W.; Stille, J. K. *J. Am. Chem. Soc.* **1974**, *96*, 4983.

(15) Nicasio, M. C.; Paneque, M.; Perez, P. J.; Pizzano, A.; Poveda, M. L.; Rey, L.; Sirol, S.; Taboada, S.; Trujillo, M.; Monge, A.; Ruiz, C.; Carmona, E. *Inorg. Chem.* **2000**, *39*, 180.

(16) Paneque, N.; Perez, P. J.; Pizzano, A.; Poveda, M. L.; Taboada, S.; Trujillo, M.; Carmona, E. *Organometallics* **1999**, *18*, 4304.

(17) Wick, D. D.; Jones, W. D. *Inorg. Chim. Acta* **2009**, *362*, 4416.

(18) (a) Tanabe, T.; Brennessel, W. W.; Clot, E.; Eisenstein, O.; Jones, W. D. *Dalton Trans.* **2010**, *39*, 10495. (b) Tanabe, T.; Evans, M. E.; Brennessel, W. W.; Jones, W. D. *Organometallics* **2011**, *30*, 834.

(19) Jiao, Y. Z.; Morris, J.; Brennessel, W. W.; Jones, W. D. *J. Am. Chem. Soc.* **2013**, *135*, 16198.

(20) (a) Stoutland, P. O.; Bergman, R. G.; Nolan, S. P.; Hoff, C. D. *Polyhedron* **1988**, *7*, 1429. (b) Stoutland, P. O.; Bergman, R. G. *J. Am. Chem. Soc.* **1988**, *110*, 5732.

(21) Campian, M. V.; Harris, J. L.; Jasim, N.; Perutz, R. N.; Marder, T. B.; Whitwood, A. C. *Organometallics* **2006**, *25*, 5093.

(22) Circu, V.; Fernandes, M. A.; Carlton, L. *Inorg. Chem.* **2002**, *41*, 3859.

(23) Campian, M. V.; Clot, E.; Eisenstein, O.; Helmstedt, U.; Jasim, N.; Perutz, R. N.; Whitwood, A. C.; Williamson, D. *J. Am. Chem. Soc.* **2008**, *130*, 4375.

(24) Cook, K. S.; Incarvito, C. D.; Webster, C. E.; Fan, Y. B.; Hall, M. B.; Hartwig, J. F. *Angew. Chem., Int. Ed.* **2004**, *43*, 5474.

(25) Callaghan, P. L.; Fernandez-Pacheco, R.; Jasim, N.; Lachaize, S.; Marder, T. B.; Perutz, R. N.; Rivalta, E.; Sabo-Etienne, S. *Chem. Commun.* **2004**, 242.

(26) (a) Braunschweig, H.; Colling, M. *Coord. Chem. Rev.* **2001**, *223*, 1. (b) Pandey, K. K. *Coord. Chem. Rev.* **2009**, *253*, 37. (c) Pandey, K. K. *Dalton Trans.* **2012**, *41*, 3278.

(27) Lachaize, S.; Sabo-Etienne, S. *Eur. J. Inorg. Chem.* **2006**, 2115.

(28) Belt, S. T.; Duckett, S. B.; Helliwell, M.; Perutz, R. N. *J. Chem. Soc., Chem. Commun.* **1989**, 928.

(29) Jones, W. D.; Partridge, M. G.; Perutz, R. N. *J. Chem. Soc., Chem. Commun.* **1991**, 264.

(30) (a) Jasim, N. A.; Perutz, R. N.; Foxon, S. P.; Walton, P. H. *J. Chem. Soc., Dalton Trans.* **2001**, 1676. (b) Bramananthan, N.; Carmona, M.; Lowe, J. P.; Mahon, M. F.; Poulten, R. C.; Whittlesey, M. K. *Organometallics* **2014**, *33*, 1986.

(31) Checinska, L.; Grabowski, S. J. *Chem. Phys.* **2006**, *327*, 202.

(32) Vicente, J.; Gil-Rubio, J.; Bautista, D.; Sironi, A.; Masciocchi, N. *Inorg. Chem.* **2004**, *43*, 5665.

(33) Macgregor, S. A.; Roe, D. C.; Marshall, W. J.; Bloch, K. M.; Bakhmutov, V. I.; Grushin, V. V. *J. Am. Chem. Soc.* **2005**, *127*, 15304.

(34) (a) Klahn, A. H.; Oelckers, B.; Godoy, F.; Garland, M. T.; Vega, A.; Perutz, R. N.; Higgitt, C. L. *J. Chem. Soc., Dalton Trans.* **1998**, 3079. (b) We explored the reaction of **6** with $Et_3N{\cdot}3HF$ (30 equiv) in THF solution and found 2.5% conversion to **7** at room temperature, increasing to 10% after heating to 60 °C for 2 h. The poor yield is consistent with weak hydrogen bonding between the RhF moiety and HF.

(35) Tp′Rh(PMe_3)(3-$C_5NH_2F_2$)H: ^{1}H NMR (C_6D_6, 300 K): δ −16.40 (ddd, J_{PH} = 29 Hz, J_{RhH} = 22 Hz, J_{FH} = 9 Hz, 1H, RhH), 1.09 (d, 9H, J_{PH} = 10 Hz, P(CH_3)$_3$). ^{19}F{^{1}H} NMR (C_6D_6): δ − 81.4 (m, 1F), −47.5 (m, 1F). ^{31}P{^{1}H} NMR (C_6D_6): δ 0.65 (dd, J_{RhP} = 137 Hz, J_{PF} = 10 Hz). Tp′Rh(PMe_3)(4-$C_5NH_2F_2$)H. ^{1}H NMR (C_6D_6, 300 K): δ −16.50 (dd, J_{PH} = 29 Hz, J_{RhH} = 25 Hz, 1H, RhH), 0.88 (d, 9H, J_{PH} = 9 Hz, P(CH_3)$_3$). ^{19}F{^{1}H} NMR (C_6D_6): δ − 67.6 (b, 2F). ^{31}P{^{1}H} NMR (C_6D_6): δ 0.70 (d, J_{RhP} = 138 Hz). Product ratio: 2:1 for activation at the 3-position.

(36) Drolet, D. P.; Lees, A. J. *J. Am. Chem. Soc.* **1992**, *114*, 4186.

(37) The importance of secondary photolysis was investigated independently. A solution of Tp′Rh(PMe_3)(Bpin)H (**2**) was irradiated in benzene solution for 6 h and the reaction followed by ^{31}P{^{1}H} NMR spectroscopy. The disappearance of the doublet for the Rh-boryl species and appearance of a new resonance for the Rh-phenyl species, confirmed that **2** absorbs at λ > 290 nm and shows photoactivity. A similar experiment performed with Tp′Rh(PMe_3)(C_5F_4N)F (**6**), however, indicated that **6** was photostable in benzene solution. Irradiation of Tp′Rh(PMe_3)(Ph)H in C_5F_5N showed formation of **6** after only a few hours of photolysis.

(38) The gradients for loss of **1** are given in the Supporting Information. They are close to one another for the three substrates but not identical. We attribute the difference to residual absorption by the substrates which was found to be greatest for pentafluoropyridine. Absorbance at 355 nm and 0.5 mm path length, 0.13 for 1.5 M pentafluoropyridine and 0.54 for 6 mM **1**.

(39) Wick, D. D.; Reynolds, K. A.; Jones, W. D. *J. Am. Chem. Soc.* **1999**, *121*, 3974.

(40) Luo, Y. *Comprehensive Handbook of Chemical Bond Energies*; CRC Press: Boca Raton, FL, 2007.

(41) Levy, C. J.; Puddephatt, R. J. *Organometallics* **1997**, *16*, 4115.

(42) Chan, D.; Duckett, S. B.; Heath, S. L.; Khazal, I. G.; Perutz, R. N.; Sabo-Etienne, S.; Timmins, P. L. *Organometallics* **2004**, *23*, 5744.

(43) Rablen, P. R.; Hartwig, J. F.; Nolan, S. P. *J. Am. Chem. Soc.* **1994**, *116*, 4121.

DOI: 10.1021/ja5113172
J. Am. Chem. Soc. 2015, 137, 1258−1272

(44) Lam, K. C.; Lin, Z. Y.; Marder, T. B. *Organometallics* **2007**, *26*, 3149.
(45) Nova, A.; Reinhold, M.; Perutz, R. N.; Macgregor, S. A.; McGrady, J. E. *Organometallics* **2010**, *29*, 1824.
(46) Zhu, J.; Lin, Z. Y.; Marder, T. B. *Inorg. Chem.* **2005**, *44*, 9384.
(47) (a) Raza, A. L.; Panetier, J. A.; Teltewskoi, M.; Macgregor, S. A.; Braun, T. *Organometallics* **2013**, *32*, 3795. (b) Teltewskoi, M.; Panetier, J. A.; Macgregor, S. A.; Braun, T. *Angew. Chem., Int. Ed.* **2010**, *49*, 3947. (c) Cronin, L.; Higgitt, C. L.; Karch, R.; Perutz, R. N. *Organometallics* **1997**, *16*, 4920.
(48) (a) Procacci, B.; Blagg, R. J.; Perutz, R. N.; Rendon, N.; Whitwood, A. C. *Organometallics* **2014**, *33*, 45. (b) Noveski, D.; Braun, T.; Neumann, B.; Stammler, A.; Stammler, H. G. *Dalton Trans.* **2004**, 4106. (c) Selmeczy, A. D.; Jones, W. D.; Partridge, M. G.; Perutz, R. N. *Organometallics* **1994**, *13*, 522.
(49) (a) Lindup, R. J.; Marder, T. B.; Perutz, R. N.; Whitwood, A. C. *Chem. Commun.* **2007**, 3664. (b) Archibald, S. J.; Braun, T.; Gaunt, J. A.; Hobson, J. E.; Perutz, R. N. *J. Chem. Soc., Dalton Trans.* **2000**, 2013.
(50) Jones, W. D. *Inorg. Chem.* **2005**, *44*, 6138.
(51) (a) Hartwig, J. F. *Acc. Chem. Res.* **2012**, *45*, 864. (b) Alcaraz, G.; Sabo-Etienne, S. *Coord. Chem. Rev.* **2008**, *252*, 2395. (c) Perutz, R. N.; Sabo-Etienne, S. *Angew. Chem., Int. Ed.* **2007**, *46*, 2578.
(52) Campian, M. V.; Perutz, R. N.; Procacci, B.; Thatcher, R. J.; Torres, O.; Whitwood, A. C. *J. Am. Chem. Soc.* **2012**, *134*, 3480.
(53) (a) Osman, R.; Perutz, R. N.; Rooney, A. D.; Langley, A. J. *J. Phys. Chem.* **1994**, *98*, 3562. (b) Colombo, M.; George, M. W.; Moore, J. N.; Pattison, D. I.; Perutz, R. N.; Virrels, I. G.; Ye, T. Q. *J. Chem. Soc., Dalton Trans.* **1997**, 2857.
(54) Evans, M. E.; Li, T.; Vetter, A. J.; Rieth, R. D.; Jones, W. D. *J. Org. Chem.* **2009**, *74*, 6907.
(55) Calladine, J. A.; Duckett, S. B.; George, M. W.; Matthews, S. L.; Perutz, R. N.; Torres, O.; Khuong, Q. V. *J. Am. Chem. Soc.* **2011**, *133*, 2303.
(56) Linden, H. B. *Eur. J. Mass Spectrom.* **2004**, *10*, 459.
(57) Dolomanov, O. V.; Bourhis, L. J.; Gildea, R. J.; Howard, J. A. K.; Puschmann, H. *J. Appl. Crystallogr.* **2009**, *42*, 339.
(58) Frieden, C. *KINSIM/FITSIM*; Washington University School of Medicine: St. Louis, MO, 1997; http://www.biochem.wustl.edu/cflab/message.html.
(59) Peng, C. Y.; Ayala, P. Y.; Schlegel, H. B.; Frisch, M. J. *J. Comput. Chem.* **1996**, *17*, 49.
(60) (a) Becke, A. D. *J. Chem. Phys.* **1993**, *98*, 1372. (b) Lee, C. T.; Yang, W. T.; Parr, R. G. *Phys. Rev. B* **1988**, *37*, 785.
(61) Frisch, M. J.; et al. *Gaussian 03*; Gaussian, Inc.: Wallingford, CT, 2004.
(62) Ehlers, A. W.; Bohme, M.; Dapprich, S.; Gobbi, A.; Hollwarth, A.; Jonas, V.; Kohler, K. F.; Stegmann, R.; Veldkamp, A.; Frenking, G. *Chem. Phys. Lett.* **1993**, *208*, 111.
(63) Hollwarth, A.; Bohme, M.; Dapprich, S.; Ehlers, A. W.; Gobbi, A.; Jonas, V.; Kohler, K. F.; Stegmann, R.; Veldkamp, A.; Frenking, G. *Chem. Phys. Lett.* **1993**, *208*, 237.
(64) Hehre, W. J.; Ditchfie, R.; Pople, J. A. *J. Chem. Phys.* **1972**, *56*, 2257.
(65) Choi, G.; Morris, J.; Brennessel, W. W.; Jones, W. D. *J. Am. Chem. Soc.* **2012**, *134*, 9276.

DOI: 10.1021/ja5113172
J. Am. Chem. Soc. 2015, 137, 1258−1272